

Variation of amino acid in the sinking particulates in the northeastern Arabian Sea and the northern Bay of Bengal

Apsara P Vijayan, Siby Kurian*, Duphrin Joseph, Megha Dixon, Harshada Kankonkar, Rakhee Khandeparker, Supriya Karapurkar, Anand Methar

¹CSIR-National Institute of Oceanography, Dona Paula, Goa, 403004, India

*Corresponding author: siby@nio.org

Phone: +91-832 2450399

Abstract

Sediment traps are widely used to get insight into how particulate matter forms and settles in the water column. Earlier studies in the Northern Indian Ocean have shown that the sinking flux depends mainly on surface primary production and varies seasonally and inter-annually. In the case of the Bay of Bengal, river runoff plays a significant role in the sinking flux. As a part of the SIBER-INDIA program, a mooring consisting of sediment traps was deployed at three depths (495 m, 1205 m, and 2915 m) in the Arabian Sea (Northeastern Arabian Sea sediment trap, NEAST; 16.87°N, 67.77°E) and at 580 m, 1110 m, and 1635 m in the Bay of Bengal (Bay of Bengal sediment trap, BoBST; 18.21°N, 89.63°E). We present here data on total fluxes, concentrations of particulate carbon and nitrogen, biogenic opal, and amino acid composition for the period 2017-2018 in both basins. Particle flux in the Arabian Sea was influenced by monsoon-related processes with higher flux during the northeast monsoon (NEM) and southwest monsoon (SWM) seasons, whereas the flux was higher in BoB during SWM. Particulate nitrogen (PN), particulate organic carbon (POC), and total hydrolysable amino acid (THAA) mostly decreased with depth in all traps due to the decomposition of labile organic constituents in the sinking flux. Changes in the decomposition of organic matter with depth were further reflected in the POC/PN molar ratios, which increased with depth in the Arabian Sea. A low POC/PN molar ratio associated with the higher THAA concentration in most of the shallow traps indicates the presence of fresher organic matter. Among the THAA, Glycine (Gly) was the dominant amino acid in all the samples followed by Aspartic acid (Asp), Glutamic acid (Glu), Serine (Ser), and Alanine (Ala). The amino acid-based degradation index (DI) reveals the degradation of labile organic matter with depth in the NEAST. However, the middle trap in the BoB showed a different trend with higher total and lithogenic fluxes, POC, PN, and DI values compared to the shallow trap indicating lateral advection in the bay. Monsoonal changes and mesoscale eddies make these basins distinct from one another and influence their sinking fluxes and biogeochemical settings.

Keywords: Sediment trap; particle flux; Arabian Sea; Bay of Bengal; amino acid; degradation index

1. Introduction:

Moored sediment traps are generally used to study the seasonal and annual changes in particle fluxes in the water column. This expanded our understanding of the dynamics of ocean particulates and their relationship to the ocean carbon cycle (Fowler et al., 2000). Studies on sediment traps revealed that the descent of particulate matter to the deep seafloor is directly associated with surface production and also a reflection of seasonality (Deuser et al., 1981; Wassman, 1984). The sediment traps were deployed in the northern Indian Ocean during the 1980s and 1990s as part of an Indo-German joint effort that disclosed that the sediment flux varies seasonally as well as inter-annually in the Arabian Sea (AS) as well as in the Bay of Bengal (BoB). The elevated sinking fluxes in these basins were associated with nutrients injected into the euphotic zone as a consequence of wind-induced deepening of the mixed layer, however, river discharge also plays an important role in the BoB (Nair et al., 1989; Ittekkot et al., 1991; Ramaswamy and Parthiban, 1992). These sediment traps were useful in monitoring the effects of the South Asian monsoon system on ocean productivity in the Indian Ocean region (Nair et al., 1989; Ittekkot et al., 1991). Both southwest monsoon (SWM, June-September) and northeast monsoon (NEM, November-February) are predominant in the northern Indian Ocean. Among them, SWM is far more energetic while NEM is characterized by weaker winds. The period intervening the monsoons, March-May and October- November are referred to as spring inter-monsoon (SIM) and fall inter-monsoon (FIM), respectively. Earlier sediment trap studies in the AS observed a substantial seasonal variation in the particle flux at all three sites (central, western, and eastern) accompanied by significant spikes during the SW and NE monsoons. However, the accuracy of the sediment trap flux studies is subject to debate. The validity of sediment trap results has been evaluated using a variety of techniques, such as reactive radionuclides as tracers and inverse modeling methods since the technique is affected by numerous hydrodynamic, biological, and chemical processes (Rixen et al., 2019a and reference therein). However, sediment traps continue to be the most often employed technique for determining the seasonal and inter-annual variability of particle fluxes in the deep ocean (Turner, 2015, Rixen et al., 2019a).

Sedimentary organic matter (OM) represents a diverse and complex mixture of organic substances with a wide variety of chemical and physical properties (Mayer et al., 1994; Hedges and Oades, 1997; Goñi et al., 1997; Hedges et al., 1997). For a better understanding of the OM burial in deep marine sediments, sediment trap-based studies are receiving more attention. Being essential components of both marine and terrestrial species, amino acid (AA) provides a considerable amount of OM to aquatic sedimentary settings (Degens and Mopper, 1976; Lee 1988; Cowie and Hedges, 1992) and delineate a considerable portion of OM preservation in recent coastal marine sediments (Keil et al., 2000). The

sediments embrace a wide range of AA forms, from small contributions of monomers to the predominance of polymeric forms including protein and humified peptide material (Gupta and Kawahata., 2000). AAs account for about one-quarter of the organic nitrogen (ON) particulates in shallow waters. Subsequent descent to the ocean floor, AAs can constitute 10 - 100% of the ON and anywhere between 1 and 50% of the organic carbon (C_{org}) in sediment. However, these proportions vary related to the origin of OM, water column depth, speed of deposition, and other variables. An appreciable quantity of AAs from marine plankton is incorporated into the sediment which usually contains 20-40% AAs by weight as the most detectable part of the OM (Lee and Cronin, 1984; Lee et al., 2004). These are often labile substances that undergo selective degradation throughout the descent in the particulate organic matter (POM) in the water column (Ittekkot et al., 1984). The primary productivity quantified in the euphotic zone at a location and AA transport through the seawater are interrelated (Lee 1988). In addition to planktonic rainout, in situ generation of C_{org} , reworking by microbes (Hutchins et al., 2017) and deposition of terrigenous material bring OM to the ocean. The OM in the sinking particles is vulnerable to various transformational and degradation changes which can cause POM to gradually change its composition while sinking (Mayers and Eadie 1993).

Variable AA fractions include total hydrolyzable amino acids (THAA), dissolved combined amino acids (DCAA), and dissolved free amino acids (DFAA). Among these, the free AAs as well as those bound to peptides and proteins constitute the THAA fraction which is particularly dominant in sediments. The AA carbon as % of total organic carbon (THAA-C), AA nitrogen as % of total nitrogen (THAA-N), and the proportion of mol % of non-protein AA such as β -alanine (β -Ala) and γ -aminobutyric acid (γ -Aba) are effective diagenetic indicators (Cowie and Hedges, 1994). During diagenetic processes, THAA is selectively decomposed or conserved and hence the yield and composition of THAA have been widely used as diagenetic indicators (Keil et al., 2000; Amon et al., 2001; Vandewiele et al., 2009).

Amino acids in the sediment trap materials were studied across different regimes for several applications. Spectral distribution of AA in the subarctic Pacific showed that OM is generally least degraded during periods of maximum particle fluxes and copepod-derived OM increases the AA in the traps (Haake et al., 1993a); an ecosystem shift from phytoplankton to a more zooplankton dominated system in Southern Kara Sea (Gaye-Haake et al., 2003); and association of AAs with biominerals in the sediment traps deployed in the Southern Ocean (Ingalls et al., 2006); and the composition of AA in the organic carbon and organic nitrogen in the sinking particles in the Potomac Estuary (Sigleo and Shultz.,1993), etc. Sediment trap investigations on AA have been carried out in the AS since 1986 at western, central, and eastern AS. Based on AA content and their spectral

distributions, Haake et al. (1992) found that the organic matter degradation in the water column is less during high-flux periods in the western and central Arabian Sea, whereas at the eastern site more degraded material of terrigenous or reworked marine origin reaches the sediment traps during late summer peak fluxes. Schäfer et al. (1996) found that the fluxes of THAA followed the seasonal variation of the total fluxes in the BoB traps with a decreasing trend with depth. Later, Gaye et al. (2013) found AA composition differs in suspended particulate matter and sinking particles in deep waters of the AS. Sinking particles are plankton-derived and exhibit progressive degradation with increasing water depth with depletion of plankton constituents and accumulation of bacterial degradation products (Gaye et al., 2013). Based on a large set of AA data (covering sinking and suspended particles, sediment samples, and dissolved AA from the water column and pore water samples), recently Gaye et al. (2022) highlighted the use of AA-derived biogeochemical indicators as proxies for organic matter sources and degradation.

Under the SIBER-INDIA program, a mooring consisting of three traps was deployed in the north-eastern Arabian Sea (NEAS) as well as northern BoB during the years 2017-2018. The objectives of this study were (i) to comprehend the seasonal changes in particle flux collected at three different depths at the NEAST and the BoBST, (ii) to study the seasonality of fluxes and their composition with reference to monsoon-related processes and mesoscale eddies, and (iii) to assess the amino acid composition and their degradation indices in the sinking flux and their controlling factors in both these basins.

2. Materials and methods

2.1. Study area

The AS is the most biologically productive region in the North Indian Ocean and also sustains one of the largest oxygen-deficient waters in the oceanic mid-depth. The two key factors that contribute to the Arabian Sea's productivity are upwelling during the SWM and winter cooling during the NEM (Ryther et al., 1966; Qasim, 1977; Berger et al., 1988). The productivity is low during inter monsoon but the bacteria-micro-meso-zooplankton loop (microbial loop) becomes active during this season (Gauns et al., 1996). A stable oxygen minimum zone (OMZ) exists in the NEAS (Naqvi et al., 1993) which lies between 150 and 1000 m depth and represents the thickest OMZ found in the world's ocean which is attributed to high surface productivity and poor ventilation of subsurface waters. A considerable fraction of total marine denitrification takes place within the AS OMZ (Codispoti et al., 2001; Bange et al., 2005). The diversity and spatio-temporal proximity of the AS make it a natural laboratory for the study of many aspects of biogeochemistry and climate change aspects such as global

warming, deoxygenation, ocean acidification, etc. The BoB is a significant location for entering freshwater and sediment input worldwide. The Bengal fan is the largest deep-sea fan in the world, and the settling particles in BoB are mostly lithogenic (river inputs) as compared to biogenic (Ittekkot et al., 1991; Gupta et al., 1997; Unger et al., 2003, 2005). The oceanographic and biological processes in BoB are strongly influenced by the monsoon. The riverine nutrient input is high during the monsoon season which can enhance primary productivity resulting in high sinking flux in the late SWM (Ittekkot et al., 1991). Apart from this mesoscale eddies also play a major role in enhancing the productivity of BoB and the observed seasonal variability in biogenic flux in the northern and central BoB (Vidya and Prasannakumar 2013; Kurian et al., 2023). An OMZ is present in BoB as well, with an upper boundary at around 60-200 m and a lower boundary at 100-800 m with a thickness of 80-650 m (Rao et al., 1994; Udaya Bhaskar et al., 2021). Based on dissolved oxygen data from the biogeochemical Argo floats, recently Udaya Bhaskar et al. (2021) reported that the OMZ is thicker in the northwestern region compared to the northeastern and southern BoB, mainly caused by stratification, higher C_{org} fluxes, and contribution from the shelf transported organic particles to the OMZ. The AS OMZ is the thickest in the world oceans and is the site of up to 40% of all denitrification, whereas the OMZ in the BoB is weaker and is not an active denitrification site (Rao et al., 1994; Bristow et al., 2017). There are several explanations put forth for the disparity in OMZ intensity between the two seas, including differences in primary productivity, distinct mesoscale eddy intensities, and diverse transport processes for OM and oxygen (McCreary et al., 2013; Udaya Bhaskar et al., 2021). The remineralization depth of BoB is deeper than that of AS, potentially interrelated with the aggregation of OM with minerals introduced from the river, which in turn weakens the OMZ in the bay (Al Azhar et al., 2017).

2.2 Sediment traps

As a part of the SIBER-INDIA program, sinking particles were collected using moored time-series sediment traps (McLane Research Laboratories Inc, USA) deployed at stations NEAST (16.87°N, 67.77°E) and BoBST (18.21 °N, 89.63°E) (Fig. 1) at a uniform sampling interval of 17 days. Three traps were deployed at BoBST (shallow: 580 m, middle: 1110 m, and deep: 1635 m) from February 2017 to February 2018. Similarly, three traps were deployed at NEAST (shallow: 495 m, middle: 1205 m, and deep: 2915 m) from October 2017 to October 2018. The deployment and retrieval of sediment traps were done onboard the research vessel *Sindhu Sankalp*. The automated traps carried 21 collection vials of 500 ml each on a motorized tray, that were filled with seawater from the deployment depths (filtered through GF/F filters and added with 33 g NaCl/L and 3.3 g HgCl₂/L (12.15 mM) to prevent diffusive processes and microbial degradation of organic matter) before the deployment. On retrieval,

the samples were labeled and refrigerated, and later sieved through a 1mm nylon sieve and separated the fraction >1mm containing larger particles. The filtrate containing particles <1mm was split into a few equal parts using a precision rotary splitter (Mclane Research Laboratories Inc., USA) and filtered onto a pre-weighed HTTP polycarbonate filter paper (0.45 μm pore size), and all chemical analyses were carried out in this fraction. One aliquot of the sample was kept at -80°C and was freeze-dried for AA analysis and others were dried at 40°C and all these aliquots were weighed to determine the total flux of <1mm. The percentage of inorganic carbon (IC) in the sample was determined using a UIC Coulometer (CM5015). Before beginning the analysis of samples, blank and CaCO_3 standards (Merck) were run in each batch. About 5 mg of dried and homogenized sediment trap samples were treated with 5ml of 1N HCl and when all the CO_2 had evolved and titrated, the value of % carbon was recorded. Periodically, a few replicates of samples and CaCO_3 standards were run to confirm the proper functioning of the instrument. The percentage of particulate inorganic carbon (PIC) in the sample was calculated using the following equation:

$$\% \text{PIC} = [(\text{display value as } \mu\text{g C}) - (\text{blank value as } \mu\text{g C})] * 100 / \text{Sample in } \mu\text{g weight}$$

$$\% \text{CaCO}_3 = \% \text{PIC} \times 100/12$$

The precision of the analysis was <2% and the accuracy was better than 1%. The total carbon (TC) and particulate nitrogen (PN) of the sediment trap samples were analyzed following Agnihotri et al. (2008) in an elemental analyzer attached to a dual-inlet isotope ratio mass spectrometer. Around 5 mg of finely ground sediment trap samples were packed in tin cups for analysis. POC was calculated by subtracting PIC from the TC of the particulate matter. The opal % was estimated following the modified method of Mortlock and Froelich (1989). About 5mg of homogenized samples were first treated with 1N HCl followed by 2% H_2O_2 to remove carbonate and organic matter, respectively. The samples were then subjected to wet alkaline extraction with 7% Na_2CO_3 at 85°C for 5 hrs followed by spectrophotometric analysis of silicate using a UV-Vis spectrophotometer at 812 nm. The calibration was done using Na_2SiF_6 . A laboratory standard (Gulf of California, GoC) was analyzed in each batch, and the precision was <2%, and the accuracy was found to be better than 4%. The opal % was calculated from the % biogenic silica by multiplying with 2.4, assuming the water content in the sample as 10% ($\text{SiO}_2 * 0.4 \text{H}_2\text{O}$) (Haake et al., 1993b, Rixen et al., 1996). The biogenic fluxes were computed based on carbonate, opal, and organic matter ($\text{POC} \times 1.8$; Francois et al., 2002) contents, whereas the lithogenic flux was calculated as the difference between the total flux and the biogenic fluxes (OM, carbonate, and biogenic opal) following Rixen et al. (2019b).

For the extraction of THAA, 50 mg of freeze-dried samples were transferred into a screw-capped glass vial followed by the addition of 6N HCl under an inert atmosphere and heated at 110°C for 24 hrs. A mixture of 2-aminobutyric acid and norvaline was added as internal standards. After hydrolysis, the sample was neutralized with 6N NaOH. The sample was then centrifuged at 6000 rpm for 4 minutes, the supernatant was then evaporated to dryness, and 2mL milli-Q water was added to dissolve the residue. This was filtered using a 0.2µm syringe filter and stored in glass vials at -80°C until analysis. A blank was also treated by following the same procedure. A fraction of the sample was then derivatized with O-phthalaldehyde (OPA) reagent and analyzed on HPLC. Analysis was performed using an Agilent 1260 Infinity HPLC and the column used was AAA (4.6x100 mm, 2.7 µm). Mobile phase A contained 10mM Na₂HPO₄ (pH 8.2) and B contained acetonitrile, methanol, and water (45:45:10) and was used as a binary solvent system to separate THAA, and the flow rate was 1.5 mL/min. Due to the presence of an amide group in the side chain of both asparagine (Asn) and glutamine (Gln), these hydrolyses to the corresponding carboxylic acids (aspartic acid (Asp) and glutamic acid (Glu)). The sum of Asp and Asn is presented here as Asp and the sum of Glu and Gln is presented as Glu in the present study. The calibration was done using the mixed amino acid standard of 17AA (Agilent advanceBio, 1 nmol/µL) comprising of Asp, glycine (Gly), alanine (Ala), valine (Val), leucine (Lue), isoleucine (Ile), serine (Ser), threonine (Thr), tyrosine (Tyr), proline (Pro), arginine (Arg), histidine (His), Glu, cysteine (Cys), phenylalanine (Phe), lysine (Lys) and methionine (Met), which is added with additional 5 AAs (Asn, Gln, tryptophan (Trp), γ-Aba, and β-Ala and 2 internal standards (norvaline (Nor) and 2-Amino butyric acid (α-Aba)). The response factor was calculated based on multiple injections and used for the quantification of samples; which showed a reproducibility of ±4% from the mean. Samples were quantified based on the area of internal standard α-Aba and finally, THAA mg/g was calculated. THAA-C% and THAA-N% were calculated based on POC and PN content. Pearson correlation with Type-II linear regression analysis was carried out to discover the interrelation among the parameters such as POC, PN, THAA, and various amino acids. The degradation index (DI) was calculated using the mol% of individual AA and the factor coefficients for the first axis of the principal component analysis (PCA) (Dauwe and Middelburg, 1998; Dauwe et al., 1999) following the formula.

$$DI = \sum_i \left[\frac{\text{vari} - \text{AVG}_{\text{vari}}}{\text{STD}_{\text{vari}}} \right] * \text{fac. coef. } i$$

where var_i is the mol% of AA_i, AVG_{vari}, and STD_{vari} are its mean and standard deviation in the data set, respectively, and fac.coef.i is the factor coefficient of AA_i based on the first axis of the PCA of AA mol%.

2.3. Satellite-derived data:

Sea surface salinity is obtained using the gridded ($0.25^\circ \times 0.25^\circ$) sea surface salinity (SSS) product from Soil Moisture and Ocean Salinity (SMOS) satellite (Boutin et al., 2020) available at [ftp://ext-catds-cecos-](ftp://ext-catds-cecos-locean:catds2010@ftp.ifremer.fr/Ocean_products/L3_DEBIAS_LOCEAN/L3_DEBIAS_LOCEAN_v5/debiasedSSS_09days_v5/)

[locean:catds2010@ftp.ifremer.fr/Ocean_products/L3_DEBIAS_LOCEAN/L3_DEBIAS_LOCEAN_v5/debiasedSSS_09days_v5/](ftp://ext-catds-cecos-locean:catds2010@ftp.ifremer.fr/Ocean_products/L3_DEBIAS_LOCEAN/L3_DEBIAS_LOCEAN_v5/debiasedSSS_09days_v5/). Monthly sea surface temperature data was obtained from Hadley Centre Sea Ice and Sea Surface Temperature data set (HadISST)

<https://www.metoffice.gov.uk/hadobs/hadisst/data/download.html> with a global spatial resolution of $1^\circ \times 1^\circ$. Monthly precipitation data were obtained from the NOAA Global Precipitation Climatology Project (GPCP). Monthly Net Primary Productivity (NPP) data were plotted using the standard product data available at the Ocean Productivity site <http://sites.science.oregonstate.edu/ocean.productivity/standard.product.php> with a spatial resolution of $0.17^\circ \times 0.17^\circ$. This data uses the Vertically Generalized Production Model (VGPM) (Behrenfeld and Falkowski, 1997) as the standard algorithm.

A 2-degree latitude-longitude grid (15.5°N - 17.5°N , 66.5°E - 68.5°E in the AS and 17.5°N - 19.5°N , 88.5°E - 90.5°E in the BoB; Fig. 1) is considered for the plots of SSS, SST, precipitation and NPP. Monthly mean sea level anomalies were downloaded from Archiving, Validation, and Interpretation of Satellite Oceanographic (AVISO) satellite altimetry data <https://www.aviso.altimetry.fr/en/data/products/sea-surface-height-products/global/gridded-sea-level-anomalies-mean-and-climatology.html>, which has a global spatial resolution of $0.25^\circ \times 0.25^\circ$. The OSCAR surface currents datasets were used for the analysis of monthly zonal and meridional sea surface currents and are available at the Asia-Pacific Data-Research Center (APDRC) <http://apdrc.soest.hawaii.edu/las/v6/dataset?catitem=2845> with a spatial resolution of $0.3^\circ \times 0.3^\circ$. Monthly vertical and horizontal components of wind were downloaded from ERA5 reanalysis datasets <https://cds.climate.copernicus.eu/cdsapp#!/dataset/reanalysis-era5-single-levels-monthly-means>. This data has a spatial resolution of $0.25^\circ \times 0.25^\circ$.

3. Results and discussion

3.1. Hydrographic conditions at the mooring sites

The monthly-averaged satellite-derived chlorophyll-*a* showed low concentration in the BoB as compared to the NEAS during 2017-2018 (Fig. 1). Monthly sea surface salinity (SSS) at the two mooring sites showed a large difference with the values ranging from 36.0 to 37.1 at the NEAST, whereas it ranged from 26.2 to 33.4 at BoBST during the deployment period (Fig. 2 a,d). The SSS varied within a narrow range at NEAST, and a sharp decline was observed during September-October

at BoBST. The sea surface temperatures (SST) were low during the NEM (26.22°C) followed by SWM with higher SST (30.19) during spring inter-monsoon (SIM) at both mooring sites (Fig. 2b,e). The monthly precipitation was higher during June (SWM) followed by December (NEM) at the NEAST location, however, the precipitation at BoB was higher from June to October (Fig. 2c,f). The climatology of SSS, SST, and precipitation are shown as green lines in Fig. 2. Though the trend is similar, the precipitation in the AS is slightly lower and BoB is higher compared to the climatology during the study period. To understand whether eddies influence the trap location, we presented the snapshots of monthly average sea level anomaly (SLA) along with surface current during the sampling period. NEAS experienced anti-cyclonic eddies during April-June however the SLA was weak (Fig. 3a). A positive SLA with anti-cyclonic eddies was seen near the BoBST during the SIM, whereas a negative SLA with cyclonic eddies was present during June-July (Fig. 3b). The NPP was maximum during August-September (SWM) followed by December-February (NEM) at NEAST and the values were low during inter-monsoon seasons (Fig. 4a). Comparing the two basins, the NPP of the Arabian Sea is three times higher (Fig. 4a) than that of BoB during SWM (Fig. 4e). The NPP showed a slight increase during SWM and NEM at the BoBST (Fig. 4e).

3.2. Seasonal variation of total and lithogenic flux in the NEAST and BoBST

The total flux of sinking particles (<1mm) ranged from 12.1 to 490.6 mg/m²/day in the shallow, 0.2 to 337.0 mg/m²/day in the middle, and 18.4 to 245.5 mg/m²/day in the deep traps at NEAST (Fig. 4 b,c,d). In the case of the shallow trap, maximum flux was recorded from the end of July to September (SWM) followed by the end of December to the middle of February (NEM; Fig. 4b). The middle trap showed a moderate flux from December to March; however, the flux was very low from April to September (Fig. 4c). This was also supported by the Recording Current Meter (RCM) deployed at 1180 m depth. During SWM, the currents were towards the northeast (away from the mooring location) which could be a reason for the low flux seen in the middle trap (*figure not shown*). The deep trap showed higher flux from August to September (SWM) followed by NEM and the lowest flux was seen during November (FIM) and April to May (SIM) (Fig. 4d). This is due to the wind-induced deepening of the mixed layer which in turn resulting into the nutrient-rich water injection to the euphotic layer from the subsurface water (Nair et al., 1989). The NPP at the trap location also showed higher values during July-August (SWM) followed by December-January (NEM) (Fig. 4a). The productivity in the Arabian Sea is mainly controlled by the upwelling during the SWM and winter cooling during the NEM (Madhupratap et al., 1996). Higher production is also aided by the supply of trace metals such as Fe through aeolian dust brought in by the monsoon winds (Sirocko and Sarnthein 1989; Banerjee and PrasannaKumar 2014; Guieu et al., 2019) as Fe limitation was reported in the AS during southwest

monsoon (Naqvi et al., 2010; Moffett et al., 2015). The climatology of NPP and present data seems to be similar during NEM and SIM, however, the NPP during SWM is higher during the study period (Fig. 4a). It is known from earlier studies that the AS has enhanced productivity for almost 8 to 9 months except during the SIM (mid-March to early SWM; Gauns et al., 2005). Hence the sinking flux at the NEAST mostly follows the seasonality of the surface productivity, except in the case of the middle trap. The lithogenic flux also recorded a similar trend of the total flux, with higher flux in the shallow (up to 198.7 mg/m²/day) and deep traps (up to 101.2 mg/m²/day) during SWM followed by NEM (up to 109.5 mg/m²/day in shallow, up to 63.8 mg/m²/day in the deep traps (Fig 5 a&c, Table 1). This shows that the vertical transport of lithogenic matter is associated with biogenic aggregate formation during the high flux period (Ramaswamy et al., 1991). The percentage of lithogenic matter didn't show much depth variation at the NEAST (Avg. 38%; Fig. 6e,j&o). Earlier studies showed that the lithogenic flux in the eastern AS is higher than the central and western AS due to the introduction of materials from the continental shelf (Ramaswamy et al., 1991; Haake et al., 1993c). The peak discharge of the Indus River is at the end of July to August and the lithogenic flux in the shallow trap was higher during this period (Fig. 5a). However, the lithogenic flux in the deep trap was higher in September (Fig. 5c) reflecting a time lag for the suspended matter from the Indus to reach the trap location (Ittekkot and Arain 1986; Ramaswamy et al., 1991). Since the material collected in the middle trap was very low during this period lithogenic flux was not computed. Apart from monsoons, mesoscale eddies can also influence the biological activities in the Arabian Sea (Fischer et al., 2002). Though an anti-cyclonic eddy was present at the mooring location during April-May 2018, the SLA was weak (~+0.2) indicating minimal eddy influence during the deployment period (Fig. 3a).

The total flux at BoBST ranged from 4.4 to 78.5 mg/m²/day in the shallow, 0.6 to 465.6 mg/m²/day in the middle, and 18 to 152.5 mg/m²/day in the deep traps (Fig. 4f,g,h). The flux in the shallow trap was comparatively higher during March-April, July-October, and January (Fig. 4f). The lithogenic flux in the shallow trap was low ranging from 2.0 to 28.7 mg/m²/day (Fig. 5d). The middle trap recorded higher flux during May and August-September, and the flux was low during the NEM (Fig. 4g). This was also supported by the RCM deployed at 824 m depth. The southward current during May favors high flux in the middle trap. However, the flux decreases during June-July, consistent with the current reversal. The flux again increases in August-September when the current is southward. During November-December, the current is northward resulting in lower flux in the trap (*figure not shown*). The lithogenic flux in the middle trap also showed higher values (118.6 to 225.6 mg/m²/day) during the same period (Fig. 5e). The total flux and lithogenic fluxes were also higher in the deep trap from May to September (Fig. 4h,5f). The percentage of lithogenic matter was higher in the middle trap (Avg.

53.6%) compared to the deep (Avg. 51%) and shallow traps (Avg. 44%; Fig. 7e,j&o). Among the three traps at BoBST, the middle trap collected more material than the shallow and deep traps during the deployment period except during the NEM of 2018. Seasonally, the NPP in the BoB is marginally higher during the SWM (July-September) and NEM compared to the inter-monsoon seasons (Fig. 4e). Nutrient supply associated with river discharge during SWM contributes to an increase in primary production in the BoB, whereas wind mixing along with eddy-pumping of nutrients enhances the primary productivity during the NEM (Prasanna Kumar et al., 2010). Due to runoff from Irrawaddy and Ganges-Brahmaputra rivers, the northern BoB has less saline water during SWM (Fig. 2d). An immense quantity of freshwater runoff ($1.5 \times 10^{12} \text{ m}^3 \text{ year}^{-1}$) along with billions of tonnes of sediment is introduced into the BoB every year (Rajawat et al., 2005; Kumar et al., 2006) whereas the AS receives only $0.3 \times 10^{12} \text{ m}^3 \text{ year}^{-1}$ (Gauns et al., 2005). Earlier studies in the BoB have shown that the particles are quickly transferred to the seabed due to an increase in the ballast with lithogenic and mineral particles in the river runoff (Ittekkot and Haake., 1990; Ittekkot et al., 1992). However, recent studies show that the export production in the BoB is less as the picophytoplankton contribute up to 75% of total phytoplankton biomass in the bay (Sarma et al., 2020) which recycles in the upper ocean, and about 50% of primary production is exudated as dissolved organic matter (Rao et al., 2021). This could be a reason for the lower flux seen in the deeper trap (Fig. 4h) at the BoBST which is deployed 500 m below the middle trap. Hence the seasonality in the flux is effected by the autochthonous production due to riverine nutrients and a significant inflow of material from rivers during the SWM. Apart from this, the bay is known for eddy activities hence mesoscale circulation may also have an impact on the sinking flux. Cyclonic eddies inject nutrients into the euphotic zone and result in increased primary production in the basin (Gomes et al., 2000; Prasanna Kumar et al., 2004). Compared to the AS, mesoscale eddies are more active in the BoB during the deployment period (Fig. 3a,b). An anti-cyclonic eddy (SLA +0.3m) was present at the mooring location during April-May 2017 and the higher flux seen in the middle and deep traps may be attributed to the influence of this downwelling eddy which is consistent with the high lithogenic flux during this period. The mooring location is also influenced by the presence of cyclonic eddies (Fig 3b). Two cyclonic eddies (SLA - 0.3m) were present near the mooring location during June-July 2017 and the current pattern shows these eddies can lead to a higher flux during this period (Fig. 4 g,h). Based on two years (2011 and 2019) of sediment trap data at BoBST, Kurian et al. (2023) reported an inter-annual variability in total and lithogenic fluxes influenced by both riverine supply and mesoscale eddies. It is evident from our study that the lithogenic percentage was higher at the BoBST (Avg. 50%) as compared to the NEAST (Avg. 38%). Hence the sinking flux at the NEAST follows the seasonality of the surface productivity whereas river discharge and mesoscale eddies largely influence the flux seen at the BoBST.

3.3. Seasonal variation in the flux composition at NEAST and BoBST

The CaCO₃ ranged from 20.9 to 52.3% in the shallow, 20.5 to 44.7% in the middle, and 29.5 to 46.1% in the deep traps at NEAST (Fig. 6 a,e,i, Table 1). Since the sample recovery was low in a few cups in the middle trap, the PIC measurements could not be carried out. The CaCO₃ ranged from 9.4 to 51.1% in the shallow, 4.7 to 33.8% in the middle, and 11.8 to 34.0% in the deep traps at BoBST (Fig. 7 a,e,i, Table 2). The CaCO₃% was higher in the NEAST as compared to the BoBST (Fig. 6&7). The CaCO₃% was higher during early SWM followed by NEM in the NEAST. Earlier sediment trap studies in the AS showed higher fluxes of CaCO₃ and C_{org} during SWM compared to the NEM (Rixen et al., 1996; Honjo et al., 1999). Coccolithophores, foraminifers, and pteropods mainly contribute to the carbonate flux in the AS, however with a spatial and seasonal variability (Guptha and Mohan 1996; Mergulhao et al., 2006; Ramaswamy and Gaye 2006). In the BoBST CaCO₃% in shallow and deep traps showed higher values in October followed by April, however, the values were low in the middle trap during October (Fig. 7 a,e,i). Earlier, Ramaswamy and Gaye (2006) observed lower foraminifera to coccolithophore ratios in the BoB at high discharge periods as foraminifera are more sensitive to saturation states. Recently Kurian et al. (2023) compared the earlier Northern Bay of Bengal Trap (NBBT-N) data with 2011 and 2019 data of BoBST and reported a decline in the carbonate flux in the BoB over the past few years due to the low saturation levels of calcite and aragonite in the water column which can lower the precipitation of carbonates within the calcifying organisms.

The opal % varied from 0.1 to 23.7 in the shallow, 5.0 to 25 in the middle, and 8.7 to 22.6 in deep traps at NEAST (Fig. 6 b,f,j, Table 1). The opal % varied from 4.7 to 20.7 in the shallow, 9.5 to 20.3 in the middle, and 14.7 to 35.5 in deep traps at BoBST (Fig. 7 b,f,j, Table 2). Higher opal % in the shallow trap (Fig. 6b) coinciding with the high flux period in the NEAST (Fig. 4b) may be due to the production and sinking of diatoms as also seen by high NPP during SWM and NEM, two highly productive periods (Fig. 4a). Corresponding to a decrease in NPP from March to June, the diatom production is also limited and is reflected in the decreased opal% in the respective samples (Fig. 6b). The NPP is comparatively higher during SWM and NEM in the BoB and the seasonality in opal % is seen in the middle and deep traps at BoBST (Fig. 7f,j). Earlier, Ittekkot et al. (2000) reported that the river runoff in BoB supplies enough silicate and can influence the phytoplankton composition in the bay, and lithogenic material acts as ballast and enhances the transport of freshly formed biogenic silica to the seafloor (Ittekkot et al., 1992). Recently, Kurian et al. (2023) reported large inter-annual variability in opal flux associated with riverine input and silicate supply which can influence the abundance of diatoms and thereby the opal flux at BoBST.

The POC % varied from 5.4 to 14.3% in shallow, 6.8 to 13.4% in the middle, and 0.6 to 7.2% in deep traps at NEAST (Fig. 6c,g,k, Table 1). It was higher in the shallow trap compared to the other two traps at NEAST. The POC varied from 3.8 to 22.9% in the shallow, 4.5 to 22.5% in the middle, and 4.3 to 11% in the deep traps at BoBST (Fig. 7c,g,k, Table 2). The POC% generally decreased with depth, however, a few samples in the middle trap showed very high values at BoBST (Fig. 7g) which also have high lithogenic fluxes (Fig. 5e). The decrease in POC% with depth in the NEAST is due to the decomposition of labile organic constituents in the sinking flux while passing through the water column (Haake et al., 1992; 1993b). The uptake of carbon by phytoplankton and its consumption by zooplankton and bacteria while exported to the deep-sea results in a decreased POC% in the deeper depths (Volk and Hoffert, 1985). Several variables such as oxygen concentration, the productivity in the upper water column, deposition rates of sediment (Stein, 1990), lithogenic introduction (Blair and Aller, 2012), and variations in the ability of different minerals to sorb OM (Keil et al., 1994; Hedges and Keil, 1995) are proposed as the governing factors for the preservation of OM. However, the trend was different in the middle trap at BoBST (Fig.7g) possibly due to lateral advection as also seen by the high lithogenic flux during SWM (Fig. 5e). Recently Shah et al. (2018) reported high dissolved organic carbon (DOC) concentration in the deeper water column in the northern bay compared to the southern region and attributed to the fresh-water influx from the Ganges-Brahmaputra rivers. Studies on Nd concentration and ϵNd (Singh et al., 2012) and dissolved silicon and $\delta^{30}\text{Si}$ (Singh et al., 2015) also showed a significant influence of this riverine system in the northern BoB. Recently Udaya Bhaskar et al. (2021) also reported the cross-shelf transport of OM in the BoB based on the particle backscatter signal from the biogeochemical Argo floats emphasizing that the OM from shelf sediments may be supporting the carbon needs in the OMZ. Hence the high POC seen in the middle trap during SWM could be mainly attributed to the contribution from riverine water during the high flux period.

In the biogeochemistry of the ocean, nitrogen has an essential role with crucial components influencing the cycles of many other elements, primarily carbon. The PN ranged from 0.7 to 2.2% in shallow, 0.9 to 1.4% in the middle (except a high value of 4.7%), and 0.7 to 1.0% in the deep trap at NEAST (Fig. 6 d,h,l, Table 1). The PN ranged from 0.5 to 3.9% for the shallow, 0.7 to 3.3% for the middle, and 0.5 to 0.9% for the deep traps at BoBST (Fig. 7d,h,l, Table 2). The PN% decreased with depth at the NEAST possibly due to the preferential utilization of nutrients while organic matter sinks through the water column (Lee and Cronin, 1982; Alldredge and Silver, 1988). Similar to POC%, the middle trap in the BoBST recorded higher PN % during the SWM whereas the shallow trap showed higher values during the NEM of 2018 (Fig. 7).

The molar POC/PN ratio varied from 6.7 to 10.5 in shallow, 3.4 to 9.2 in the middle, and 0.7 to 11.0 in deep traps at NEAST (Table 1). However, the ratios showed a wide range with higher values for the middle and deep traps at BoBST. The ratio varied from 6.7 to 16.6 in shallow, 5.4 to 25.2 in the middle, and from 7.0 to 19.9 in the deep traps at BoBST (Table 2). The POC/PN molar ratios in the NEAST fall in the range of algal-derived organic matter whereas few samples in the middle and deep traps at BoBST showed higher ratios during the SWM. Recently, Sarma et al. (2020) reported that picophytoplankton contributes up to 75% of total phytoplankton biomass in the BoB, however, their export production is not very high as they remineralize in the upper water column. Hence, the presence of terrestrial vascular plant remnants reaching the water column during high precipitation periods could be responsible for high POC/PN molar ratios in the middle trap of BoB. This is also supported by the high lithogenic flux in the middle trap during this season (Fig. 5). The shallow traps at NEAST and BoBST were deployed in the OMZ and the degradation of organic matter is less in the OMZ compared to the degradation rate while passing through the oxic water column due to reduced bacterial activity and lowered zooplankton activity (Cram et al., 2021). Similar results were found in the South Pacific Ocean where POC fluxes were constant with depth within the suboxic waters of the Peru oxygen deficient zone while stations with no suboxic waters showed decreasing POC flux in the same depth range (Pavia et al., 2019).

3.4 Seasonal variation of amino acids in the NEAST and BoBST

THAA (mg/g) ranged from 7.5 to 30.0 mg/g in the shallow, 5.5 to 10.7 mg/g in the middle, and 3.1 to 6.6 mg/g in the deep traps at NEAST (Fig. 8, Table 1). The THAA concentration ranged from 6.4 to 29.9 mg/g in shallow, 9.2 to 86 mg/g in the middle, and 4.3 to 10.8 in deep traps at BoBST (Fig. 9, Table 2). Similar to POC and PN, the THAA concentrations in both basins decrease with depth, except in a few samples of the middle trap at BoBST (Fig. 9). The THAA content has been used as a diagenetic indicator due to their preferential preservation or decomposition during the phase of diagenesis (Keil et al., 2000; Amon et al., 2001), thus their decrease with increasing depth in NEAST denotes the degradation of organic matter along the trajectory. Also, POC (mg/g) and PN (mg/g) showed a positive correlation with THAA (mg/g) at both sites possibly confirming that the increase or decrease in the organic matter directly influences the amino acid concentrations. The correlation of POC (mg/g) and THAA (mg/g) showed R values of 0.85, $p < 0.01$, $n = 36$ and 0.57, $p < 0.01$, $n = 32$, respectively for NEAST and BoBST samples. Similarly, the correlation of PN (mg/g) and THAA (mg/g) showed R values of 0.88, $p < 0.01$, $n = 36$, and 0.55, $p < 0.01$, $n = 32$ for NEAST and BoBST (Tables 5&6). A low molar POC/PN ratio in the shallow trap is associated with higher THAA concentration. In contrast, a higher

ratio in the deep trap is associated with lower THAA concentration, indicating organic matter freshness decreases with depth (Tables 1&2).

The amount of C_{org} characterized as amino acid carbon (THAA-C%) and the portion of PN represented by amino acid nitrogen (THAA-N%) are widely used to evaluate the degree of degradation of sedimentary organic matter due to the labile nature of THAA. The THAA-C% and THAA-N% decreased with depth at the NEAST (Fig. 8) and BoBST (Fig. 9) except for one sample in the middle trap of BoBST. As expected, the percentages of THAA-C and THAA-N were low in deep traps due to the labile nature of amino acids (Degens and Mopper, 1976; Henrichs et al, 1984; Cowie and Hedges, 1992). Among the THAA, Gly, Ala, Asp, Glu, Phe, Ser, Leu, Lys, and Arg were relatively higher in all the samples at NEAST and BoBST. The average mol% of amino acid in the shallow, middle, and deep traps are shown in Fig. 10.

Fresh plankton-originated amino acids such as Leu, Lys, and Phe concentrations decreased with depth in both basins indicating depletion of the organic matter with increasing depth (Dauwe et al., 1999). The positive correlation seen between Leu and Lys with biogenic silica in these samples showed the role of these amino acids in the production of biogenic silica in the diatoms (Baio et al., 2014). The negatively charged amino acids, Asp and Glu were dominant after Gly in all depths (Fig. 10). These AAs are abundant in carbonate skeletons (Degens 1976) and are absorbed primarily into carbonates (Carter and Mitterer, 1978). The positive correlation between Asp and Glu ($R=0.78$, $p<0.01$, $n=36$ at NEAST and 0.59 , $p<0.01$, $n=32$ at BoBST (Tables 5&6) reveals the resemblance of these compounds which undergo comparable enzymatic and chemical decarboxylation and deamination processes. Since Asp are richer in calcareous organisms and Gly is that of siliceous organisms, Asp to Gly ratio may reveal the main biological sources of proteins and amino acids in the samples (Zhang et al., 2020). Also, Asp to Gly ratio >2 in the sediment trap sample indicates calcareous organisms' enrichment (Ittekkot et al., 1984). This ratio varied from 0.30 to 0.88 (except for one high value of 4.96) in the shallow, 0.28 to 0.80 in the middle, and 0.20 to 0.61 in the deep traps at NEAST (Fig. 11). The ratio varies from 0.19 to 0.81 in the shallow 0.27 to 1.15 in the middle and 0.26 to 1.04 in deep traps at BoBST, indicating the samples are not enriched with calcareous organisms. The diatom and coccolithophore dominance in OM formulated two biogeochemical indicator amino acids, as the sum of Ser and Thr (mol%) and the Asp/Gly ratio can be used to refer to the diatomaceous and calcareous sources of C_{org} in samples (Gupta and Kawahata., 2000). A plot of Ser+Thr (mol%) against Asp/Gly ratios indicates that samples collected from both basins are dominated by diatomaceous organic matter compared to calcareous sources, except one higher Asp/Gly ratio (4.96) in a shallow sample of NEAST (Fig. 11). Though the $CaCO_3\%$ is nearly double the biogenic opal % in these traps, the amino

acid-based plot indicates diatom dominance. This indicates that diatom cell walls act as an important carrier for organic carbon flux to the deep ocean as they are resistant to heterotrophic reworking (Salter et al., 2010). Similar observations were found by Salter et al. (2010) in sediment trap samples collected from the northeast Atlantic. The earlier studies showed the diatom dominance in phytoplankton composition in the NEAS (Sawant and Madhupratap 1996, Vijayan et al., 2021., Chndrasekhararao et al., 2022) and BoB (Madhupratap et al., 2003; Paul et al., 2008).

Tyrosine is usually enriched in the cell plasma of diatoms and is easily susceptible to degradation (Dauwe and Middelburg, 1998). The average mol% of Tyr was low in the deep trap at NEAST, whereas it remained almost the same among the traps at the BoBST (Fig. 10). The decrease in organic matter freshness while sinking to the seafloor can be seen in the NEAST while BoBST has an additional source of OM in the deeper depths as seen by the higher POC, PN, and THAA during SWM. Tyr shows a significant positive correlation with PN ($R=0.37$, $p<0.05$, $n=36$) and THAA ($R=0.42$, $p<0.05$, $n=36$) in the NEAST, but the correlation is insignificant for the BoBST (Tables 5&6).

The average concentration of Gly (mol%) increased from 15.0 in shallow to 18.3 in the middle to 23.0 in deep traps at NEAST. The average mol% of Gly was 16.1 in shallow, 13.9 in the middle, and 18.6 in deep traps at BoBST (Fig. 10). The increase in mol% of Gly with depth not only suggests the degradation of organic matter but more importantly, it suggests the degradation of other amino acids that are more labile (Dauwe et al., 1999; Keil et al., 2000). This is because Gly can be produced from an array of other amino acids as a remnant of heterotrophic metabolism (Dauwe and Middelburg 1998; Goodfriend 2000). Compared to shallow and middle traps, the mol% of Val was higher in deep traps (5.14 and 4.60 for NEAST and BoBST, respectively, Tables 3&4). Val is a common amino acid produced by bacteria and also produced in peptidoglycan (Perez 2003), confirming the bacterial-mediated degradation in the deeper traps in both basins. Similarly, a neutral AA Ile also showed an increase in concentration with depth in the NEAST. THAA is negatively correlated with Ile with an $R= -0.55$, $p<0.01$, $n=36$ (Table 5) which indicates that the concentration of Ile increases with degraded OM. Since a large quantity of neutral amino acids is a sign of degraded protein, and in turn the degraded OM (Sigleo et al., 1983), the increment in Ile with depth thus reveals the degradation pattern of sinking particles with depth in the AS. However, the trend was different in the BoBST with a higher concentration of Ile in the middle trap compared to other traps (Fig. 10).

Nonprotein amino acids β -Ala and γ -Aba were present in very low concentrations in a few samples of NEAST during the end of NEM and inter monsoons in the shallow trap, and γ -Aba were present in almost all samples in the middle trap (Table 3). β -Ala was present in a few samples at BoBST during SIM and early SWM, whereas γ -Aba was below the detection limit throughout the sampling period

(Table 4). It is reported that the β -Ala and γ -Aba are decomposition products of Asp and Glu, respectively, which means the carboxylation reactions result in the addition of β -Ala and γ -Aba (Lee and Cronin 1982, Ittekkot et al., 1984). The concentration of β -Ala and γ -Aba were below the detection limit during the high flux period at NEAST and BoBST. Based on a sediment trap study conducted in the Sargasso Sea, Ittekkot et al. (1984) also found a low concentration of β -Ala during the high flux seasons. They found less degraded organic matter in the trap which is just below the euphotic zone during the high flux periods due to high primary productivity at the surface. The presence of Met in the shallow trap in the Arabian Sea follows a similar trend as that of β -Ala and γ -Aba which also appears during the low flux period.

Amino acid-based DI is effective for the characterization of the diagenetic status of marine sediments, which covers a wide range of degradation states (Dauwe et al., 1999). Several studies have demonstrated that the DI is a reliable index to determine the degree of diagenetic change in sediments (Dauwe and Middelburg, 1998., Keil et al., 2000; Vandewiele et al., 2009; Fernandes et al., 2014; Salas et al., 2018), sinking material (Unger et al., 2005, Salter et al., 2010, Gaye et al., 2013; 2022) and suspended particulate matter (SPM) (Gaye et al., 2013; 2022). Though DI values can vary depending on the nature of samples (Davis and Benner, 2005) it has been widely used to understand the degradation state of the OM. The DI values ranged from -4.20 to 3.60 at the NEAST and -6.02 to 2.52 at BoBST (Fig. 12 a&b), where positive values suggest less degradation and negative ones signify more. The DI values were high (0.31 to 3.60) in the shallow trap compared to the middle (-4.2 to 0.59) and deep traps (-2.91 to 1.22) in the NEAST (Fig. 12a). High positive DI values were found in the shallow trap at the NEAST during the SWM indicating the introduction of freshly produced (less degraded) organic matter into the basin during this period, whereas the low values in the middle and deep traps reflected the degradation of OM while descending through the water column. However, the deep trap showed a few positive values during the NEM.

On the other hand, the DI followed a different pattern at BoBST with no systematic trend for the shallow, middle, and deep traps (Fig. 12b). The DI values ranged from -4.73 to 1.14 in the shallow trap, -0.84 to 2.08 in the middle trap and -6.03 to 2.52 in the deep traps at BoBST. The middle and deep traps at BoBST showed more positive DI values compared to the shallow trap during the SWM, indicating lateral advection of fresh riverine input into the deep sea during the peak flux period. Earlier, Salter et al. (2010) also found high POC fluxes, lithogenic fluxes, and DI values during the high flux period in a sediment trap deployed at North East Atlantic, and emphasized that the lithogenic fluxes can act as highly significant mediators of organic carbon transfer to the deep ocean. The ballast effect due to the lithogenic matter is also higher in the BoB which can reduce the OM degradation while

sinking through the water column. It is evident from the present study that the amino acid-based DI is not that effective in the BoB where lithogenic fluxes are dominant, whereas it is a better proxy for organic matter degradation in the Arabian Sea.

4. Conclusion

Based on sediment trap data from the AS and BoB, our study reveals that the monsoon-induced primary production leads to higher fluxes at different depths in the water column. The sinking flux at the NEAST follows the seasonality of the surface productivity with higher flux during SWM followed by NEM. At the BoBST the total fluxes were higher during the SWM, and the middle trap collected more material showing lateral advection of riverine particulates. Lithogenic fluxes, percentages of POC and PN, and their ratios were also higher in the middle trap during SWM indicating the presence of higher vascular plant remnants in the particle flux. Apart from riverine runoff, mesoscale eddies also seem to have contributed to the higher flux seen at the BoBST. Among the THAA, Gly, Asp, Glu, Ser, Thr, and Ala were dominant in the trap samples whereas β -Ala and γ -Aba were absent during the high flux period. Our study shows that amino acid-based DI can be used as a proxy for OM degradation in the AS, however, it is not effective in the BoB where lithogenic fluxes are dominant. Since mesoscale eddies and lateral advection of riverine particles influence the sinking flux in the BoB, more studies based on isotopic (radiogenic and stable) and biomarker proxies are recommended to understand the effect of anthropogenic perturbations on the basin.

Acknowledgment:

We thank the Director CSIR-NIO for his support and encouragement. We are grateful to the Biogeochemistry group, Chief Scientists, and the entire scientific team and crew of mooring cruises for their help and assistance. We acknowledge the help received from Ms. Krishnendu P and Ms. Snehal Gauns during the laboratory analyses. We thank Dr. Akhil V. and Dr. Albertina Dias for their help during the manuscript revision. This study was carried out as a part of the SIBER-INDIA (GAP-2425) project funded by the Ministry of Earth Sciences, New Delhi, with ship time support from CSIR-NIO. This is NIO contribution No: XXXX.

References

Agnihotri, R., Kurian, S., Fernandes, M., Reshma, K., D'Souza, W., & Naqvi, S. W. A. (2008). Variability of subsurface denitrification and surface productivity in the coastal eastern Arabian Sea over the past seven centuries. *The Holocene*, 18(5), 755–764. <https://doi.org/10.1177/0959683608091795>

- Al Azhar, M., Lachkar, Z., Lévy, M., & Smith, S. (2017). Oxygen Minimum Zone Contrasts Between the Arabian Sea and the Bay of Bengal Implied by Differences in Remineralization Depth. *Geophysical Research Letters*, 44(21). Portico. <https://doi.org/10.1002/2017gl075157>
- Allredge, A. L., & Silver, M. W. (1988). Characteristics, dynamics, and significance of marine snow. *Progress in Oceanography*, 20(1), 41–82. [https://doi.org/10.1016/0079-6611\(88\)90053-5](https://doi.org/10.1016/0079-6611(88)90053-5)
- Amon, R. M. W., Fitznar, H.-P., & Benner, R. (2001). Linkages among the bioreactivity, chemical composition, and diagenetic state of marine dissolved organic matter. *Limnology and Oceanography*, 46(2), 287–297. Portico. <https://doi.org/10.4319/lo.2001.46.2.0287>
- Baio, J. E., Zane, A., Jaeger, V., Roehrich, A. M., Lutz, H., Pfaendtner, J., Drobný, G. P., & Weidner, T. (2014). Diatom Mimics: Directing the Formation of Biosilica Nanoparticles by Controlled Folding of Lysine-Leucine Peptides. *Journal of the American Chemical Society*, 136(43), 15134–15137. <https://doi.org/10.1021/ja5078238>
- Banerjee, P., and S. Prasanna Kumar (2014), Dust-induced episodic phytoplankton blooms in the Arabian Sea during winter monsoon, *J.Geophys. Res. Oceans*,119, 7123–7138,doi:10.1002/2014JC010304
- Bange, H. W., Naqvi, S. W. A., & Codispoti, L. A. (2005). The nitrogen cycle in the Arabian Sea. *Progress in Oceanography*, 65(2–4), 145–158. <https://doi.org/10.1016/j.pocean.2005.03.002>
- Behrenfeld, M. J., & Falkowski, P. G. (1997). Photosynthetic rates derived from satellite-based chlorophyll concentration. *Limnology and Oceanography*, 42(1), 1–20. Portico. <https://doi.org/10.4319/lo.1997.42.1.0001>
- Berger, W.H., 1988. Ocean carbon flux: global maps of primary production and export production. *Biogeochemical cycling and fluxes between the deep euphotic zone and other oceanic realms.*, 88, pp.131-176.
- Blair, N. E., & Aller, R. C. (2012). The Fate of Terrestrial Organic Carbon in the Marine Environment. *Annual Review of Marine Science*, 4(1), 401–423. <https://doi.org/10.1146/annurev-marine-120709-142717>
- Boutin Jacqueline, Vergely Jean-Luc, Khvorostyanov Dmitry (2020). SMOS SSS L3 maps generated by CATDS CEC LOCEAN. debias V5.0. SEANOE. <http://doi.org/10.17882/52804#79565>
- Bristow L A, Callbeck C M, Larsen M, Altabet M A, Dekaezemaeker J, Forth M, Gauns M, Glud R N, Kuypers M M, Lavik G, Milucka J, Naqvi S W A, Pratihary A, Revsbech N P, Thamdrup B, Treusch A H and Canfield D E 2017 N₂ production rates limited by nitrite availability in the Bay of Bengal oxygen minimum zone; *Nat. Geosci.* 10 24–29
- Carter, P. W., & Mitterer, R. M. (1978). Amino acid composition of organic matter associated with carbonate and non-carbonate sediments. *Geochimica et Cosmochimica Acta*, 42(8), 1231–1238. [https://doi.org/10.1016/0016-7037\(78\)90116-3](https://doi.org/10.1016/0016-7037(78)90116-3).
- Chndrasekhararao, AV. Kurian, S., Vidya, P.J., Gauns, M., (2022). Seasonal and inter-annual variability of chemotaxonomic marker pigments in the north-eastern Arabian Sea, *Deep Sea Research-1*, 179, 103679.

- Codispoti, L. A., Brandes, J. A., Christensen, J. P., Devol, A. H., Naqvi, S. W. A., Paerl, H. W., & Yoshinari, T. (2001). The oceanic fixed nitrogen and nitrous oxide budgets: Moving targets as we enter the anthropocene? *Scientia Marina*, 65(S2), 85–105. <https://doi.org/10.3989/scimar.2001.65s285>
- Cowie, G. L., & Hedges, J. I. (1992). Sources and reactivities of amino acids in a coastal marine environment. *Limnology and Oceanography*, 37(4), 703–724. Portico. <https://doi.org/10.4319/lo.1992.37.4.0703>
- Cowie, G. L., & Hedges, J. I. (1994). Biochemical indicators of diagenetic alteration in natural organic matter mixtures. *Nature*, 369(6478), 304–307. <https://doi.org/10.1038/369304a0>
- Cram, J., Fuchsman, C., Duffy, M., Pretty, J., Lekanoff, R., Neibauer, J., Leung, S., Huebert, K.B., Weber, T., Bianchi, D., 2021. Slow particle remineralization, rather than suppressed disaggregation, drives efficient flux transfer through the Eastern Tropical North Pacific Oxygen Deficient Zone. *Earth and Space Science Open Archive ESSOAr*.
- Dauwe, B., & Middelburg, J. J. (1998). Amino acids and hexosamines as indicators of organic matter degradation state in North Sea sediments. *Limnology and Oceanography*, 43(5), 782–798. Portico. <https://doi.org/10.4319/lo.1998.43.5.0782>
- Dauwe, B., Middelburg, J. J., Herman, P. M. J., & Heip, C. H. R. (1999). Linking diagenetic alteration of amino acids and bulk organic matter reactivity. *Limnology and Oceanography*, 44(7), 1809–1814. Portico. <https://doi.org/10.4319/lo.1999.44.7.1809>
- Davis, J., & Benner, R. (2005). Seasonal trends in the abundance, composition and bioavailability of particulate and dissolved organic matter in the Chukchi/Beaufort Seas and western Canada Basin. *Deep Sea Research Part II: Topical Studies in Oceanography*, 52(24–26), 3396–3410. <https://doi.org/10.1016/j.dsr2.2005.09.006>
- Degens, E. T. 1976. Molecular mechanisms on carbonate, phosphate, and silica deposition in the living cell. *Top. Curr. Chem.* 64: 1–112, doi:10.1007/BFb0045698
- Degens, E. T., & Mopper, K. (1976). Factors Controlling the Distribution and Early Diagenesis of Organic Material in Marine Sediments. *Chemical Oceanography*, 59–113. <https://doi.org/10.1016/b978-0-12-588606-2.50012-6>
- Deuser, W. G., Ross, E. H., & Anderson, R. F. (1981). Seasonality in the supply of sediment to the deep Sargasso Sea and implications for the rapid transfer of matter to the deep ocean. *Deep Sea Research Part A. Oceanographic Research Papers*, 28(5), 495–505. [https://doi.org/10.1016/0198-0149\(81\)90140-0](https://doi.org/10.1016/0198-0149(81)90140-0)
- Fernandes, L., Garg, A., & Borole, D. V. (2014). Amino acid biogeochemistry and bacterial contribution to sediment organic matter along the western margin of the Bay of Bengal. *Deep Sea Research Part I: Oceanographic Research Papers*, 83, 81–92. <https://doi.org/10.1016/j.dsr.2013.09.006>
- Fischer, A. S., Weller, R. A., Rudnick, D. L., Eriksen, C. C., Lee, C. M., Brink, K. H., Fox, C. A., & Leben, R. R. (2002). Mesoscale eddies, coastal upwelling, and the upper-ocean heat budget in the Arabian Sea. *Deep Sea Research Part II: Topical Studies in Oceanography*, 49(12), 2231–2264. [https://doi.org/10.1016/s0967-0645\(02\)00036-x](https://doi.org/10.1016/s0967-0645(02)00036-x)

- Fowler, S. W., Noshkin, V. E., Jacques La, R., & Gastaud, J. (2000). Temporal variations in plutonium and americium inventories and their relation to vertical transport in the northwestern Mediterranean Sea. *Limnology and Oceanography*, 45(2), 446–458. Portico. <https://doi.org/10.4319/lo.2000.45.2.0446>
- Francois, R., Honjo, S., Krishfield, R., & Manganini, S. (2002). Factors controlling the flux of organic carbon to the bathypelagic zone of the ocean. *Global Biogeochemical Cycles*, 16(4), 34–1–34–20. <https://doi.org/10.1029/2001gb001722>
- Gauns, M., Madhupratap, M., Ramaiah, N., Jyothibabu, R., Fernandes, V., Paul, J. T., & Prasanna Kumar, S. (2005). Comparative accounts of biological productivity characteristics and estimates of carbon fluxes in the Arabian Sea and the Bay of Bengal. *Deep Sea Research Part II: Topical Studies in Oceanography*, 52(14–15), 2003–2017. <https://doi.org/10.1016/j.dsr2.2005.05.009>
- Gauns, M., Mohanraju, R. and Madhupratap, M., 1996. Studies on the microzooplankton from the central and eastern Arabian Sea. *Current Science*, 71(11).
- Gaye, B., Lahajnar, N., Harms, N., Paul, S. A. L., Rixen, T., & Emeis, K.-C. (2022). What can we learn from amino acids about oceanic organic matter cycling and degradation? *Biogeosciences*, 19(3), 807–830. <https://doi.org/10.5194/bg-19-807-2022>
- Gaye, B., Nagel, B., Dähnke, K., Rixen, T., Lahajnar, N., & Emeis, K.-C. (2013). Amino acid composition and $\delta^{15}\text{N}$ of suspended matter in the Arabian Sea: implications for organic matter sources and degradation. *Biogeosciences*, 10(11), 7689–7702. <https://doi.org/10.5194/bg-10-7689-2013>
- Gaye-Haake, B., Unger, D., Nöthig, E., Okolodkov, Y.B., Fahl, K., & Ittekkot, V. (2003). Particle fluxes from short-term sediment trap deployments in late summer in the southern Kara Sea.
- Gomes, H. R., Goes, J. I., & Saino, T. (2000). Influence of physical processes and freshwater discharge on the seasonality of phytoplankton regime in the Bay of Bengal. *Continental Shelf Research*, 20(3), 313–330. [https://doi.org/10.1016/s0278-4343\(99\)00072-2](https://doi.org/10.1016/s0278-4343(99)00072-2)
- Goñi, M. A., Ruttenger, K. C., & Eglinton, T. I. (1997). Sources and contribution of terrigenous organic carbon to surface sediments in the Gulf of Mexico. *Nature*, 389(6648), 275–278. <https://doi.org/10.1038/38477>
- Goodfriend, G.A., Collins, M., Fogel, M., Macko, S. and Wehmiller, J.F. eds., 2000. *Perspectives in amino acid and protein geochemistry*. Oxford University Press, USA
- Guieu, C., Al Azhar, M., Aumont, O., Mahowald, N., Levy, M., Ethé, C., Lachkar, Z., (2019) Major impact of dust deposition on the productivity of the Arabian Sea, *Geophys. Res. Lett.*, 46 (12) 6736-6744. Gupta, L. P., & Kawahata, H. (2000). Amino acid and hexosamine composition and flux of sinking particulate matter in the equatorial Pacific at 175°E longitude. *Deep Sea Research Part I: Oceanographic Research Papers*, 47(10), 1937–1960. [https://doi.org/10.1016/s0967-0637\(00\)00009-1](https://doi.org/10.1016/s0967-0637(00)00009-1)
- Guptha, M. V. S., & Mohan, R. (1996). Seasonal variability of the vertical fluxes of *Globigerina bulloides* (d'Orbigny) in the northern Indian Ocean.

- Guptha, M. V. S., Curry, W. B., Ittekkot, V., & Muralinath, A. S. (1997). Seasonal variation in the flux of planktic Foraminifera; sediment trap results from the Bay of Bengal, northern Indian Ocean. *The Journal of Foraminiferal Research*, 27(1), 5–19. <https://doi.org/10.2113/gsjfr.27.1.5>
- Haake, B., Ittekkot, V., Honjo, S., & Manganini, S. (1993a). Amino acid, hexosamine and carbohydrate fluxes to the deep subarctic Pacific (Station P). *Deep Sea Research Part I: Oceanographic Research Papers*, 40(3), 547–560. [https://doi.org/10.1016/0967-0637\(93\)90145-s](https://doi.org/10.1016/0967-0637(93)90145-s)
- Haake, B., Ittekkot, V., Ramaswamy, V., Nair, R. R., & Honjo, S. (1992). Fluxes of amino acids and hexosamines to the deep Arabian Sea. *Marine Chemistry*, 40(3–4), 291–314. [https://doi.org/10.1016/0304-4203\(92\)90028-9](https://doi.org/10.1016/0304-4203(92)90028-9)
- Haake, B., Ittekkot, V., Rixen, T., Ramaswamy, V., Nair, R. R., & Curry, W. B. (1993b). Seasonality and interannual variability of particle fluxes to the deep Arabian sea. *Deep Sea Research Part I: Oceanographic Research Papers*, 40(7), 1323–1344. [https://doi.org/10.1016/0967-0637\(93\)90114-i](https://doi.org/10.1016/0967-0637(93)90114-i)
- Haake, B., Rixen, T. and Ittekkot, V., 1993c. Variability of monsoonal upwelling signals in the deep western Arabian Sea. *SCOPE/UNEP Sonderband*, 76, pp.85-96.
- Hedges, J. I., & Keil, R. G. (1995). Sedimentary organic matter preservation: an assessment and speculative synthesis. *Marine Chemistry*, 49(2–3), 81–115. [https://doi.org/10.1016/0304-4203\(95\)00008-f](https://doi.org/10.1016/0304-4203(95)00008-f)
- Hedges, J. I., & Oades, J. M. (1997). Comparative organic geochemistries of soils and marine sediments. *Organic Geochemistry*, 27(7–8), 319–361. [https://doi.org/10.1016/s0146-6380\(97\)00056-9](https://doi.org/10.1016/s0146-6380(97)00056-9)
- Hedges, J. I., Keil, R. G., & Benner, R. (1997). What happens to terrestrial organic matter in the ocean? *Organic Geochemistry*, 27(5–6), 195–212. [https://doi.org/10.1016/s0146-6380\(97\)00066-1](https://doi.org/10.1016/s0146-6380(97)00066-1)
- Henrichs, S. M., Farrington, J. W., & Lee, C. (1984). Peru upwelling region sediments near 15°S. 2. Dissolved free and total hydrolyzable amino acids1. *Limnology and Oceanography*, 29(1), 20–34. Portico. <https://doi.org/10.4319/lo.1984.29.1.0020>
- Honjo, S., Dymond, J., Prell, W., & Ittekkot, V. (1999). Monsoon-controlled export fluxes to the interior of the Arabian Sea. *Deep Sea Research Part II: Topical Studies in Oceanography*, 46(8–9), 1859–1902. [https://doi.org/10.1016/s0967-0645\(99\)00047-8](https://doi.org/10.1016/s0967-0645(99)00047-8)
- Hutchins, D. A., & Fu, F. (2017). Microorganisms and ocean global change. *Nature Microbiology*, 2(6). <https://doi.org/10.1038/nmicrobiol.2017.58>
- Ingalls, A.E., Liu, Z., Lee, C (2006), Seasonal trends in the pigment and amino acid compositions of sinking particles in biogenic CaCO₃ and SiO₂ dominated regions of the Pacific sector of the Southern Ocean along 170°W, *Deep Sea Research Part I: Oceanographic Research Papers*, 53, 836-859

- Ittekkot, V., & Arain, R. (1986). Nature of particulate organic matter in the River Indus, Pakistan. *Geochimica et Cosmochimica Acta*, 50(8), 1643–1653. [https://doi.org/10.1016/0016-7037\(86\)90127-4](https://doi.org/10.1016/0016-7037(86)90127-4)
- Ittekkot, V., & Haake, B. (1990). The Terrestrial Link in the Removal of Organic Carbon in the Sea. *Facets of Modern Biogeochemistry*, 318–325. https://doi.org/10.1007/978-3-642-73978-1_25
- Ittekkot, V., Deuser, W. G., & Degens, E. T. (1984). Seasonality in the fluxes of sugars, amino acids, and amino sugars to the deep ocean: Sargasso Sea. *Deep Sea Research Part A. Oceanographic Research Papers*, 31(9), 1057–1069. [https://doi.org/10.1016/0198-0149\(84\)90012-8](https://doi.org/10.1016/0198-0149(84)90012-8)
- Ittekkot, V., Haake, B., Bartsch, M., Nair, R. R., & Ramaswamy, V. (1992). Organic carbon removal in the sea: the continental connection. Geological Society, London, Special Publications, 64(1), 167–176. <https://doi.org/10.1144/gsl.sp.1992.064.01.11>
- Ittekkot, V., Humborg, C., & Schäfer, P. (2000). Hydrological Alterations and Marine Biogeochemistry: A Silicate Issue? *BioScience*, 50(9), 776. [https://doi.org/10.1641/0006-3568\(2000\)050\[0776:haamba\]2.0.co;2](https://doi.org/10.1641/0006-3568(2000)050[0776:haamba]2.0.co;2)
- Ittekkot, V., Nair, R. R., Honjo, S., Ramaswamy, V., Bartsch, M., Manganini, S., & Desai, B. N. (1991). Enhanced particle fluxes in Bay of Bengal induced by injection of fresh water. *Nature*, 351(6325), 385–387. <https://doi.org/10.1038/351385a0>
- Keil R G, Tsamakis E, Hedges J I (2000) *Amino Acid and Protein Geochemistry*; Oxford University Press, New York. pp. 69-82.
- Keil, R. G., Montluçon, D. B., Prahl, F. G., & Hedges, J. I. (1994). Sorptive preservation of labile organic matter in marine sediments. *Nature*, 370(6490), 549–552. <https://doi.org/10.1038/370549a0>
- Kumar, V.S., Pathak, K.C., Pednekar, P.N.S.N., Raju, N.S.N. and Gowthaman, R., 2006. Coastal processes along the Indian coastline. *Current science*, pp.530-536 <https://www.jstor.org/stable/24093957>
- Kurian, S., Shenoy, D. M., V.P, A., Kessarkar, P. M., Gauns, M., Shetye, S. S., Kabeer, M., Vijayan, A. P., Methar, A., Karapurkar, S., Chndrasekhararao, A. V., & Naqvi, S. W. A. (2023). Spatial and seasonal variations in the particulate sinking flux in the Bay of Bengal. *Progress in Oceanography*, 211, 102983. <https://doi.org/10.1016/j.pocean.2023.102983>
- Lee, C. and Cronin, C., 1982. The vertical flux of particulate organic nitrogen in the sea: decomposition of amino acids in the Peru upwelling area and the equatorial Atlantic. *J. mar. Res*, 40(1), pp.227-251.
- Lee, C., & Cronin, C. (1984). Particulate amino acids in the sea: Effects of primary productivity and biological decomposition. *Journal of Marine Research*, 42(4), 1075–1097. <https://doi.org/10.1357/002224084788520710>
- Lee, C., 1988. Amino acid and amine biogeochemistry in marine particulate material and sediments. *Nitrogen cycling in coastal marine environments*, pp.125-141.

- Lee, C., Wakeham, S., & Arnosti, C. (2004). Particulate Organic Matter in the Sea: The Composition Conundrum. *AMBIO: A Journal of the Human Environment*, 33(8), 565–575. <https://doi.org/10.1579/0044-7447-33.8.565>
- Madhupratap, M., Gauns, M., Ramaiah, N., Prasanna Kumar, S., Muraleedharan, P. M., de Sousa, S. N., Sardesai, S., & Muraleedharan, U. (2003). Biogeochemistry of the Bay of Bengal: physical, chemical and primary productivity characteristics of the central and western Bay of Bengal during summer monsoon 2001. *Deep Sea Research Part II: Topical Studies in Oceanography*, 50(5), 881–896. [https://doi.org/10.1016/s0967-0645\(02\)00611-2](https://doi.org/10.1016/s0967-0645(02)00611-2)
- Madhupratap, M., Kumar, S. P., Bhattathiri, P. M. A., Kumar, M. D., Raghukumar, S., Nair, K. K. C., & Ramaiah, N. (1996). Mechanism of the biological response to winter cooling in the northeastern Arabian Sea. *Nature*, 384(6609), 549–552. <https://doi.org/10.1038/384549a0>
- Mayer, L. M. (1994). Surface area control of organic carbon accumulation in continental shelf sediments. *Geochimica et Cosmochimica Acta*, 58(4), 1271–1284. [https://doi.org/10.1016/0016-7037\(94\)90381-6](https://doi.org/10.1016/0016-7037(94)90381-6)
- Mayer PA, Eadie BJ (1993) Sources, degradation and recycling of organic matter associated with sinking particles in Lake Michigan. *Org Geochem* 20:47-56
- McCreary, J. P., Yu, Z., Hood, R. R., Vinayachandran, P. N., Furue, R., Ishida, A., & Richards, K. J. (2013). Dynamics of the Indian-Ocean oxygen minimum zones. *Progress in Oceanography*, 112-113, 15–37. <https://doi.org/10.1016/j.pocean.2013.03.002>
- Mergulhao, L. P., Mohan, R., Murty, V. S. N., Guptha, M. V. S., & Sinha, D. K. (2006). Coccolithophores from the central Arabian Sea: Sediment trap results. *Journal of Earth System Science*, 115(4), 415–428. <https://doi.org/10.1007/bf02702870>
- Moffett, J.W., Vedamati, J., Goepfert, T.J., Pratihary, A.K., Gauns, M., Naqvi, S.W.A. (2015), Biogeochemistry of iron in the Arabian Sea, *Limnol. Oceanogr.* 60, 1671-1688
- Mortlock, R.A., Froelich, P.N., 1989. A simple method for the rapid determination of biogenic opal in pelagic marine sediments. *Deep Sea Res.* 36 (9), 1415–1426
- Nair, R. R., Ittekkot, V., Manganini, S. J., Ramaswamy, V., Haake, B., Degens, E. T., Desai, B. N., & Honjo, S. (1989). Increased particle flux to the deep ocean related to monsoons. *Nature*, 338(6218), 749–751. <https://doi.org/10.1038/338749a0>
- Naqvi, S. W. A., Kumar, M. D., Narvekar, P. V., De Sousa, S. N., George, M. D., & D’Silva, C. (1993). An intermediate nepheloid layer associated with high microbial metabolic rates and denitrification in the northwest Indian Ocean. *Journal of Geophysical Research*, 98(C9), 16469. <https://doi.org/10.1029/93jc00973>
- Naqvi, S. W. A., Moffett, J.W., Gauns, M., Narvekar, P.V., Pratihary, A.K., Naik, H., Shenoy, D.M, Jayakkumar, D.A, Geopfert, T.J., Patra P.K., Al-Azri, A., Ahmed, S.I., (2010). The Arabian Sea as a high nutrient, low-chlorophyll region during the late Southwest Monsoon. *Biogeosciences*, 7: 2091–2100. doi: 10.5194/bg-7-2091-2010
- Paul, J. T., Ramaiah, N., & Sardesai, S. (2008). Nutrient regimes and their effect on distribution of phytoplankton in the Bay of Bengal. *Marine Environmental Research*, 66(3), 337–344. <https://doi.org/10.1016/j.marenvres.2008.05.007>

- Pavia, F. J., Anderson, R. F., Lam, P. J., Cael, B. B., Vivancos, S. M., Fleisher, M. Q., Lu, Y., Zhang, P., Cheng, H., & Edwards, R. L. (2019). Shallow particulate organic carbon regeneration in the South Pacific Ocean. *Proceedings of the National Academy of Sciences*, 116(20), 9753–9758. <https://doi.org/10.1073/pnas.1901863116>
- Perez, M.T., Pausz, C. & Herndl, G.J., 2003. Major shift in bacterioplankton utilization of enantiomeric amino acids between surface waters and the ocean's interior. *Limnology and Oceanography*, 48, 755-763. <https://doi.org/10.4319/lo.2003.48.2.0755>
- Prasanna Kumar, S., Narvekar, J., Nuncio, M., Kumar, A., Ramaiah, N., Sardesai, S., Gauns, M., Fernandes, V. and Paul, J., 2010. Is the biological productivity in the Bay of Bengal light limited? *Current science*, pp.1331-1339.
- Prasanna Kumar, S., Nuncio, M., Narvekar, J., Kumar, A., Sardesai, D.S., De Souza, S.N., Gauns, M., Ramaiah, N. and Madhupratap, M., 2004. Are eddies nature's trigger to enhance biological productivity in the Bay of Bengal? *Geophysical Research Letters*, 31(7). <https://doi.org/10.1029/2003gl019274>
- Qasim SZ (1977) Biological productivity of the Indian Ocean. *Indian J Mar Sci* 6:122–137
- Rajawat, A.S., Gupta, M., Pradhan, Y., Thomaskutty, A.V. and Nayak, S., 2005. Coastal processes along the Indian Coast-Case studies based on synergistic use of IRS-P4 OCM and IRS1C/1D data
- Ramaswamy, V., & Gaye, B. (2006). Regional variations in the fluxes of foraminifera carbonate, coccolithophorid carbonate and biogenic opal in the northern Indian Ocean. *Deep Sea Research Part I: Oceanographic Research Papers*, 53(2), 271–293. <https://doi.org/10.1016/j.dsr.2005.11.003>
- Ramaswamy, V., Nair, R. R., Manganini, S., Haake, B., & Ittekkot, V. (1991). Lithogenic fluxes to the deep Arabian sea measured by sediment traps. *Deep Sea Research Part A. Oceanographic Research Papers*, 38(2), 169–184. [https://doi.org/10.1016/0198-0149\(91\)90078-t](https://doi.org/10.1016/0198-0149(91)90078-t)
- Ramaswamy, V., Parthiban, G. (1992). Particle fluxes in the Bay of Bengal measured by sediment traps. *Bay of Bengal and the Andaman Sea, Seminar, Calcutta, Geol. Surv. India Spec. Publ.*, 29, 25-32
- Rao, C.K., S.W.A. Naqvi, M.D. Kumar, S.J.D. Varaprasad, D.A. Jayakumar, M.D. George, and S.Y.S. Singbal. 1994. Hydrochemistry of the Bay of Bengal: Possible reasons for a different water-column cycling of carbon and nitrogen from the Arabian Sea. *Marine Chemistry* 47:279–290, [http://dx.doi.org/10.1016/0304-4203\(94\)90026-4](http://dx.doi.org/10.1016/0304-4203(94)90026-4).
- Rao, D. N., Chopra, M., Rajula, G. R., Durgadevi, D. S. L., & Sarma, V. V. S. S. (2021). Release of significant fraction of primary production as dissolved organic carbon in the Bay of Bengal. *Deep-Sea Research I*, 168, 103445. <https://doi.org/10.1016/j.dsr.2020.103445>
- Rixen, T., Gaye, B., & Emeis, K.-C. (2019a). The monsoon, carbon fluxes, and the organic carbon pump in the northern Indian Ocean. *Progress in Oceanography*, 175, 24–39. <https://doi.org/10.1016/j.pocean.2019.03.001>

- Rixen, T., Gaye, B., Emeis, K.-C., & Ramaswamy, V. (2019b). The ballast effect of lithogenic matter and its influences on the carbon fluxes in the Indian Ocean. *Biogeosciences*, 16(2), 485–503. <https://doi.org/10.5194/bg-16-485-2019>
- Rixen, T., Haake, B., Ittekkot, V., Gupta, M. V. S., Nair, R. R., & Schlüssel, P. (1996). Coupling between SW monsoon-related surface and deep ocean processes as discerned from continuous particle flux measurements and correlated satellite data. *Journal of Geophysical Research: Oceans*, 101(C12), 28569–28582. Portico. <https://doi.org/10.1029/96jc02420>
- Ruttenberg, K. C., & Goñi, M. A. (1997). Phosphorus distribution, C:N:P ratios, and $\delta^{13}\text{C}_{\text{oc}}$ in arctic, temperate, and tropical coastal sediments: tools for characterizing bulk sedimentary organic matter. *Marine Geology*, 139(1–4), 123–145. [https://doi.org/10.1016/s0025-3227\(96\)00107-7](https://doi.org/10.1016/s0025-3227(96)00107-7)
- Ryther, J. H., Hall, J. R., Pease, A. K., Bakun, A., & Jones, M. M. (1966). Primary organic production in relation to the chemistry and hydrography of the western Indian ocean. *Limnology and Oceanography*, 11(3), 371–380. Portico. <https://doi.org/10.4319/lo.1966.11.3.0371>
- Salas, P. M., Sujatha, C. H., Ratheesh Kumar, C. S., & Cheriyan, E. (2018). Amino acids as indicators to elucidate organic matter degradation profile in the Cochin estuarine sediments, Southwest coast of India. *Marine Pollution Bulletin*, 127, 273–284. <https://doi.org/10.1016/j.marpolbul.2017.12.010>
- Salter, I., Kemp, A. E. S., Lampitt, R. S., & Gledhill, M. (2010). The association between biogenic and inorganic minerals and the amino acid composition of settling particles. *Limnology and Oceanography*, 55(5), 2207–2218. Portico. <https://doi.org/10.4319/lo.2010.55.5.2207>
- Sarma, V.V.S.S., Chopra, M., Rao, D.N., Priya, M.M.R., Rajula, G.R., Lakshmi, D.S.R., Rao, V.D., (2020) Role of eddies on controlling total and size-fractionated primary production in the Bay of Bengal, *Continental Shelf Research*, 204; 104186
- Sawant, S. and Madhupratap, M., 1996. Seasonality and composition of phytoplankton. *Current Science*, 71(11).
- Schäfer, P., V. Ittekkot, M. Bartsch, R. R. Nair, and J. Tiemann, Fresh water influx and particle flux variability in the Bay of Bengal, in *Particle Flux in the Ocean*, SCOPE, vol. 57, pp. 271–292, edited by V. Ittekkot et al., John Wiley, New York, p. 372, 1996
- Shah, C., Sudheer, A. K., & Bhushan, R. (2018). Distribution of dissolved organic carbon in the Bay of Bengal: Influence of sediment discharge, fresh water flux, and productivity. *Marine Chemistry*, 203, 91–101. <https://doi.org/10.1016/j.marchem.2018.04.004>
- Sigleo, A. C., & Shultz, D. J. (1993). Amino Acid Composition of Suspended Particles, Sediment-Trap Material, and Benthic Sediment in the Potomac Estuary. *Estuaries*, 16(3), 405. <https://doi.org/10.2307/1352588>
- Sigleo, A. C., Hare, P. E., & Helz, G. R. (1983). The amino acid composition of estuarine colloidal material. *Estuarine, Coastal and Shelf Science*, 17(1), 87–96. [https://doi.org/10.1016/0272-7714\(83\)90047-1](https://doi.org/10.1016/0272-7714(83)90047-1)

- Singh, S. P., Singh, S. K., Goswami, V., Bhushan, R., & Rai, V. K. (2012). Spatial distribution of dissolved neodymium and ϵNd in the Bay of Bengal: Role of particulate matter and mixing of water masses. *Geochimica et Cosmochimica Acta*, 94, 38–56. <https://doi.org/10.1016/j.gca.2012.07.017>
- Singh, S. P., Singh, S. K., Bhushan, R., & Rai, V. K. (2015). Dissolved silicon and its isotopes in the water column of the Bay of Bengal: Internal cycling versus lateral transport. *Geochimica et Cosmochimica Acta*, 151, 172–191. <https://doi.org/10.1016/j.gca.2014.12.019>
- Sirocko, F., & Sarnthein, M. (1989). Wind-Borne Deposits in the Northwestern Indian Ocean: Record of Holocene Sediments Versus Modern Satellite Data. *Paleoclimatology and Paleometeorology: Modern and Past Patterns of Global Atmospheric Transport*, 401–433. https://doi.org/10.1007/978-94-009-0995-3_17
- Stein, R. (1990). Organic carbon content/sedimentation rate relationship and its paleoenvironmental significance for marine sediments. *Geo-Marine Letters*, 10(1), 37–44. <https://doi.org/10.1007/bf02431020>
- Turner, J. T. (2015). Zooplankton fecal pellets, marine snow, phytodetritus and the ocean's biological pump. *Progress in Oceanography*, 130, 205–248. <https://doi.org/10.1016/j.pocean.2014.08.005>.
- Udaya Bhaskar, T. V. S., Sarma, V. V. S. S., & Pavan Kumar, J. (2021). Potential mechanisms responsible for spatial variability in intensity and thickness of oxygen minimum zone in the Bay of Bengal. *Journal of Geophysical Research: Biogeosciences*, 126, e2021JG006341. <https://doi.org/10.1029/2021JG006341>
- Unger, D., Ittekkot, V., Schäfer, P., & Tiemann, J. (2005). Biogeochemistry of particulate organic matter from the Bay of Bengal as discernible from hydrolysable neutral carbohydrates and amino acids. *Marine Chemistry*, 96(1–2), 155–184. <https://doi.org/10.1016/j.marchem.2004.12.005>
- Unger, D., Ittekkot, V., Schäfer, P., Tiemann, J., & Reschke, S. (2003). Seasonality and interannual variability of particle fluxes to the deep Bay of Bengal: influence of riverine input and oceanographic processes. *Deep Sea Research Part II: Topical Studies in Oceanography*, 50(5), 897–923. [https://doi.org/10.1016/s0967-0645\(02\)00612-4](https://doi.org/10.1016/s0967-0645(02)00612-4)
- Vandewiele, S., Cowie, G., Soetaert, K., & Middelburg, J. J. (2009). Amino acid biogeochemistry and organic matter degradation state across the Pakistan margin oxygen minimum zone. *Deep Sea Research Part II: Topical Studies in Oceanography*, 56(6–7), 376–392. <https://doi.org/10.1016/j.dsr2.2008.05.035>
- Vidya, P. J., & Kumar, S. P. (2013). Role of mesoscale eddies on the variability of biogenic flux in the northern and central Bay of Bengal. *Journal of Geophysical Research: Oceans*, 118(10), 5760–5771. <https://doi.org/10.1002/jgrc.20423>
- Vijayan, A. K., Reddy, B. B., Sudheesh, V., Marathe, P. H., Nampoothiri, V. N., Harikrishnachari, N. V., Kavya, P., Gupta, G. V. M., & Ramanamurthy, M. V. (2021). Phytoplankton community structure in a contrasting physico-chemical regime along the eastern Arabian Sea during the winter monsoon. *Journal of Marine Systems*, 215, 103501. <https://doi.org/10.1016/j.jmarsys.2020.103501>

Volk, T., & Hoffert, M. I. (1985). Ocean Carbon Pumps: Analysis of Relative Strengths and Efficiencies in Ocean-Driven Atmospheric CO₂ Changes. *Geophysical Monograph Series*, 99–110. <https://doi.org/10.1029/gm032p0099>

Wassmann, P. (1984). Sedimentation and benthic mineralization of organic detritus in a Norwegian fjord. *Marine Biology*, 83(1), 83–94. <https://doi.org/10.1007/bf00393088>

Zhang, K., Zou, L., Dai, Q., Wang, J., Jiang, X., & Liang, S. (2020). Impact of Water-Sediment Regulation on Variations of Amino Acids in the Middle-Lower Yellow River, China. *Journal of Ocean University of China*, 19(2), 369–376. <https://doi.org/10.1007/s11802-020-4159-0>

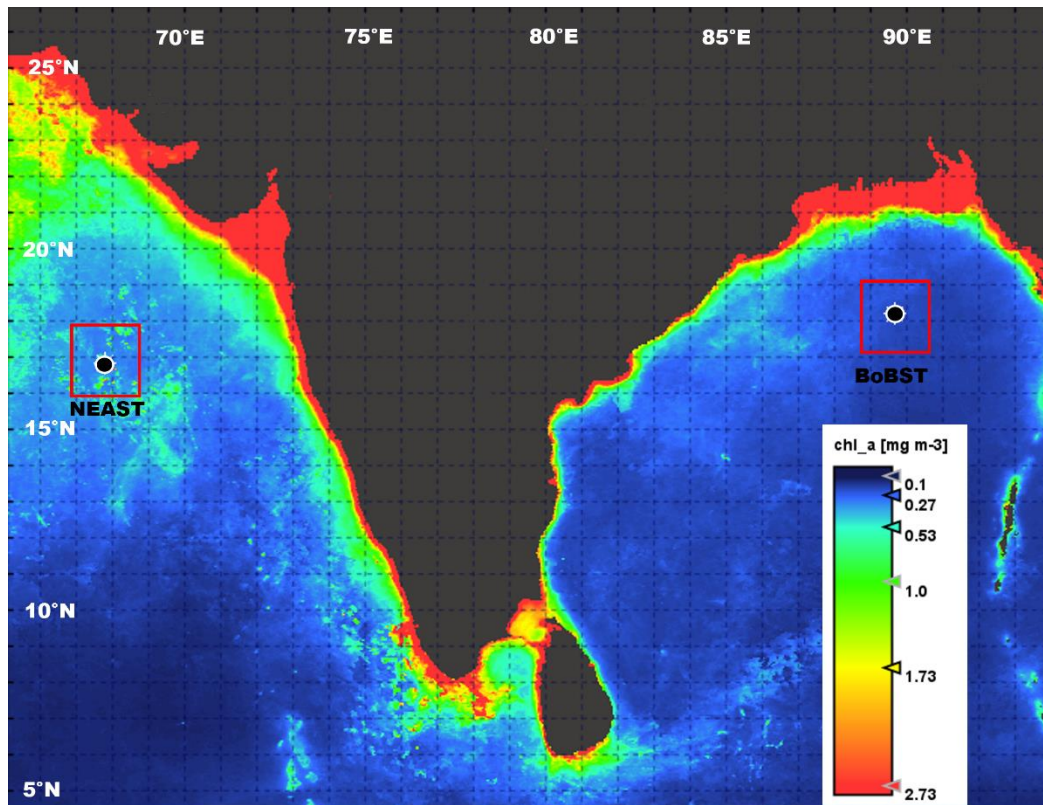


Figure 1. The monthly-averaged satellite derived chlorophylla (mg m^{-3}) during 2017-2018. The sediment trap mooring locations of NEAST (16.87°N , 67.77°E) and BoBST (18.21°N , 89.63°E) in the Arabian Sea and the Bay of Bengal are shown as black filled circles. The red color square denotes the area (2-degree latitude-longitude grid) considered for the time series plots of SSS, SST, precipitation and NPP.

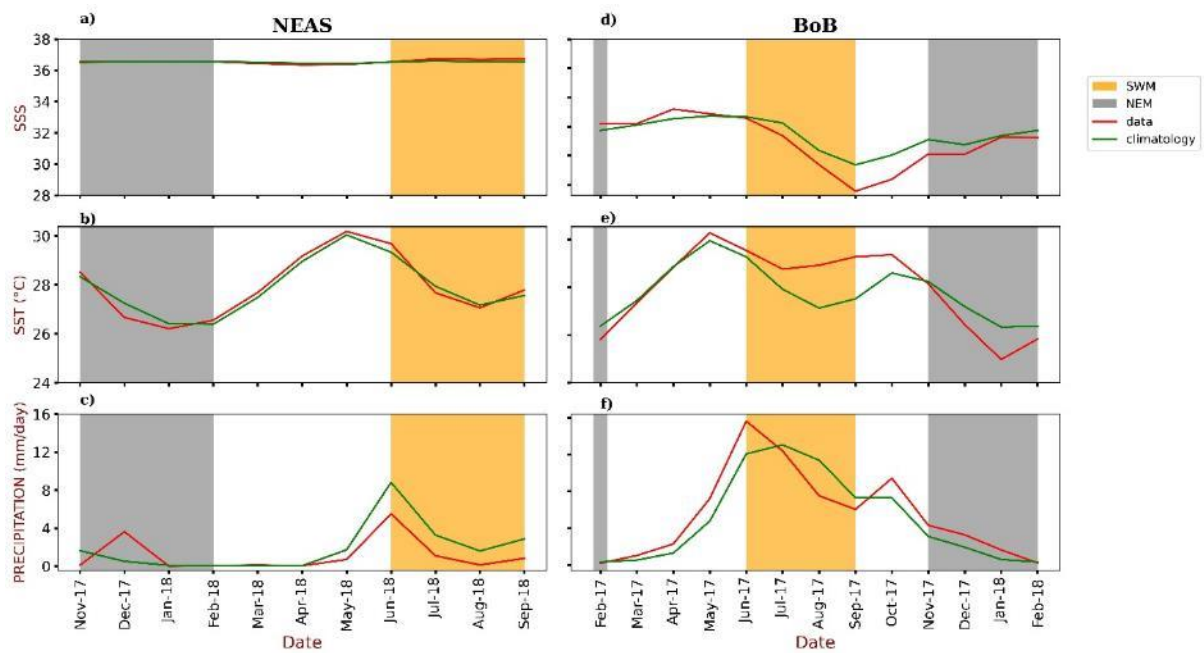


Figure 2. Time series of sea surface salinity (SSS), sea surface temperature (SST), and precipitation averaged over the red box shown in Fig.1 in the NEAS (LHS) and northern BoB (RHS). The red line indicates present data during 2017-2018 whereas the green line denotes the climatology. The climatology of SSS is derived from 2010 to 2020, whereas SST and precipitation data is for 2000 to 2020. The SWM and NEM are denoted as shaded boxes.

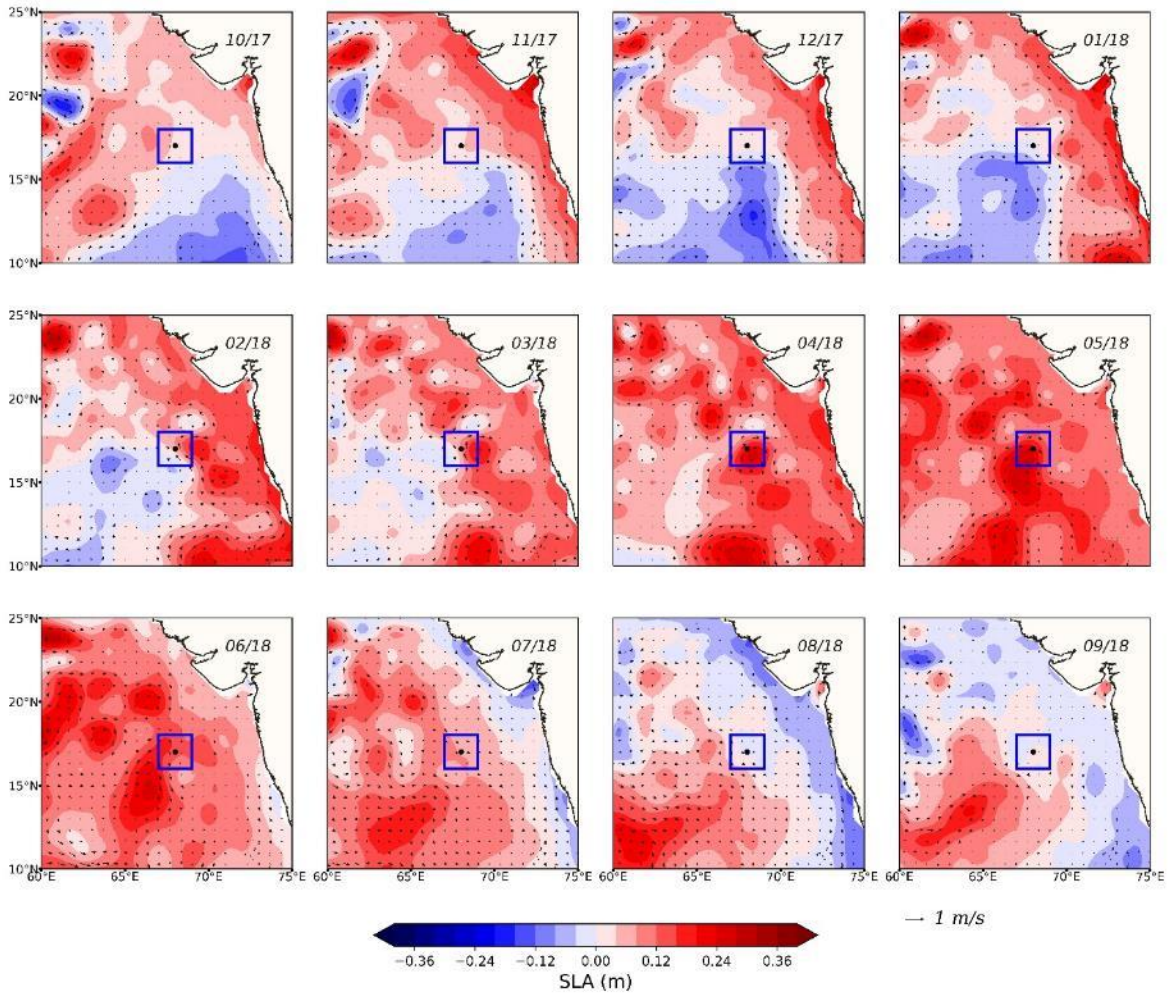


Figure 3a. Snapshots of monthly average sea level anomaly (color) and GEKCO surface current (vector) in the NEAS during October 2017 to September 2018. The sediment trap location is shown inside the blue box.

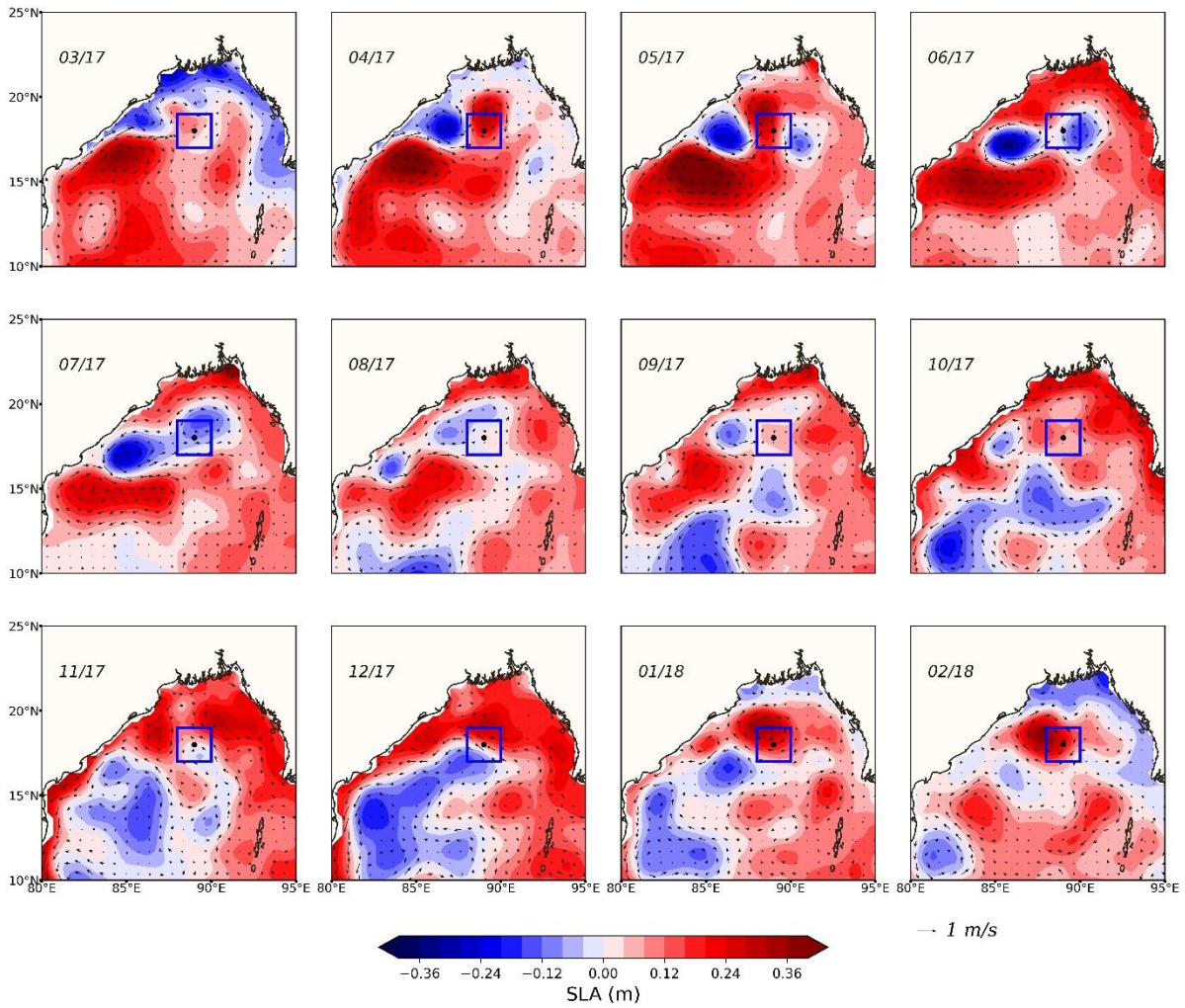


Figure 3b. Snapshots of monthly average sea level anomaly (color) and GEKCO surface current (vector) in the northern BoB during March 2017 to February 2018. The sediment trap location is shown inside the blue box.

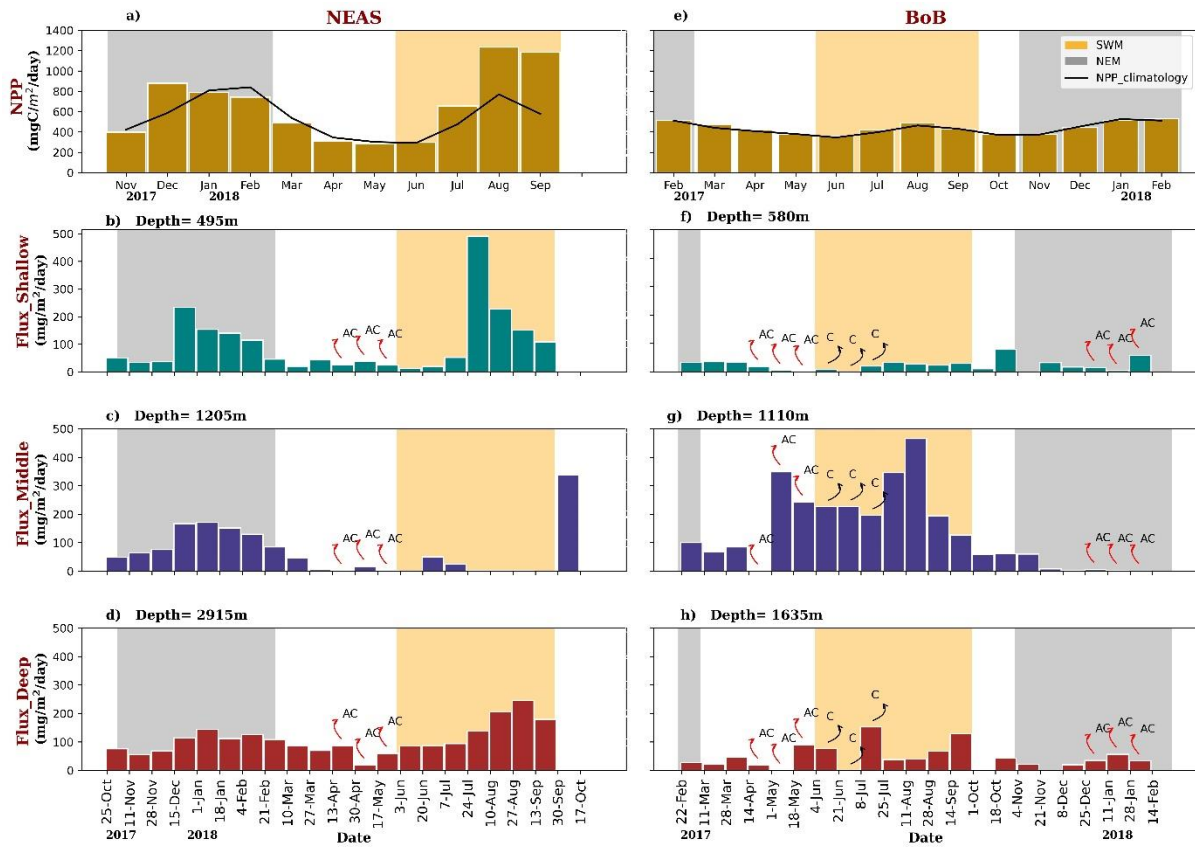


Figure 4. Net primary productivity (NPP) in the (a) NEAS and (e) BoB averaged over the box shown in Fig.1. The black line denotes the climatology of NPP during 2002-2022. Total fluxes collected in (b) shallow, (c) middle and (d) deep traps in the NEAST from October 2017 to September 2018 (LHS); and (f) shallow, (g) middle and (h) deep traps in the BoBST from February 2017 to February 2018 (RHS). Cyclonic (C) and anti-cyclonic (AC) eddies are shown as arrows and SWM and NEM are denoted as shaded boxes.

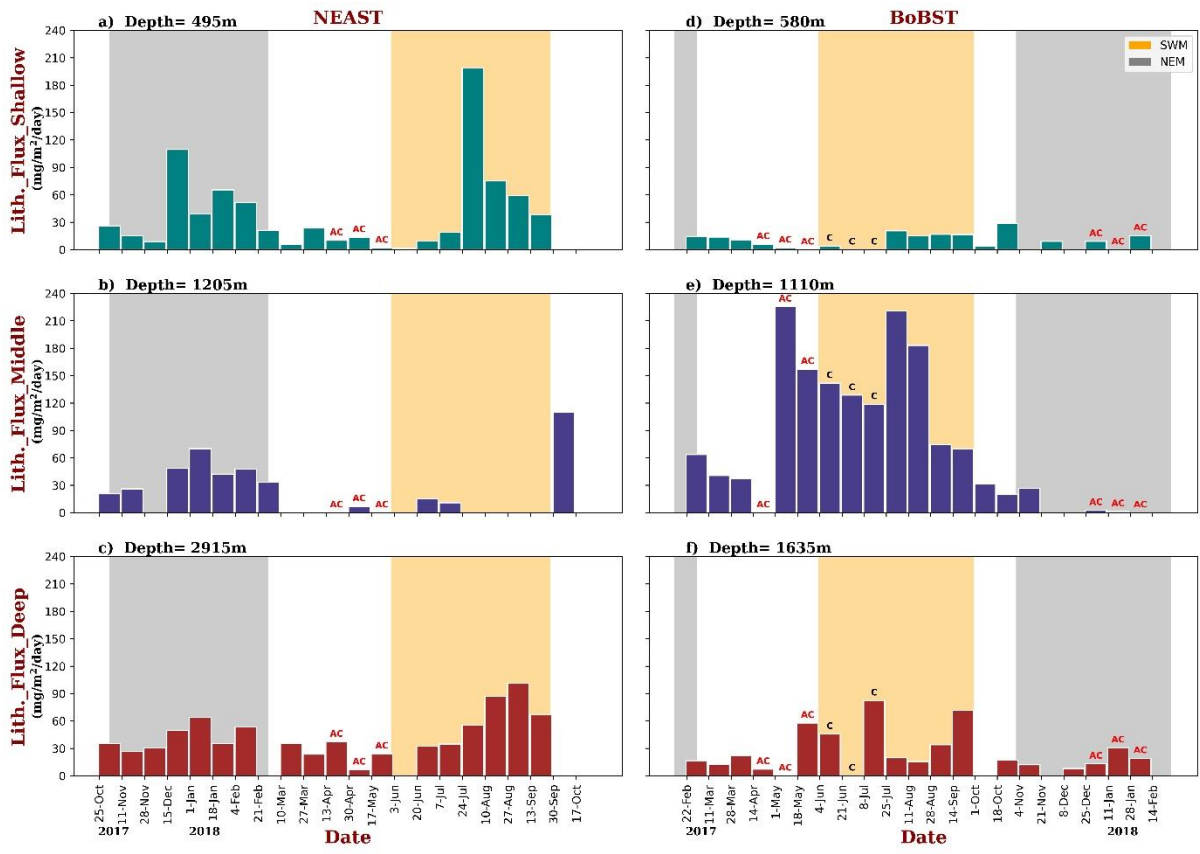


Figure 5. Seasonal variation of lithogenic fluxes collected in (a) shallow, (b) middle and (c) deep traps in the NEAST from October 2017 to September 2018 (LHS); and (d) shallow, (e) middle and (f) deep traps in the BoBST from February 2017 to February 2018 (RHS). Cyclonic (C) and anti-cyclonic (AC) eddies are shown and SWM and NEM are denoted as shaded boxes.

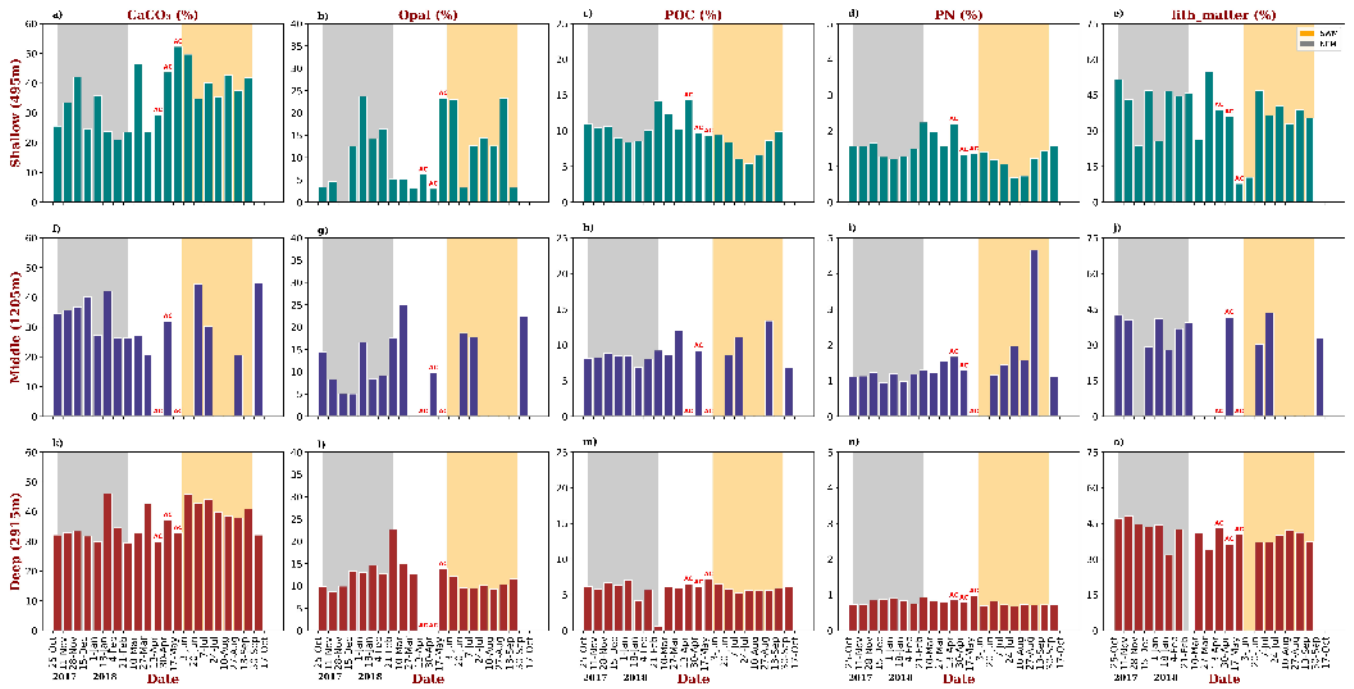


Figure 6. Seasonal variations of $\text{CaCO}_3\%$, Opal%, POC%, PN% and lithogenic matter% in the shallow (a-e), middle (f-j) and deep (k-o) traps in the NEAST from October 2017 to October 2018. Cyclonic (C) and anti-cyclonic (AC) eddies are shown and SWM and NEM are denoted as shaded boxes.

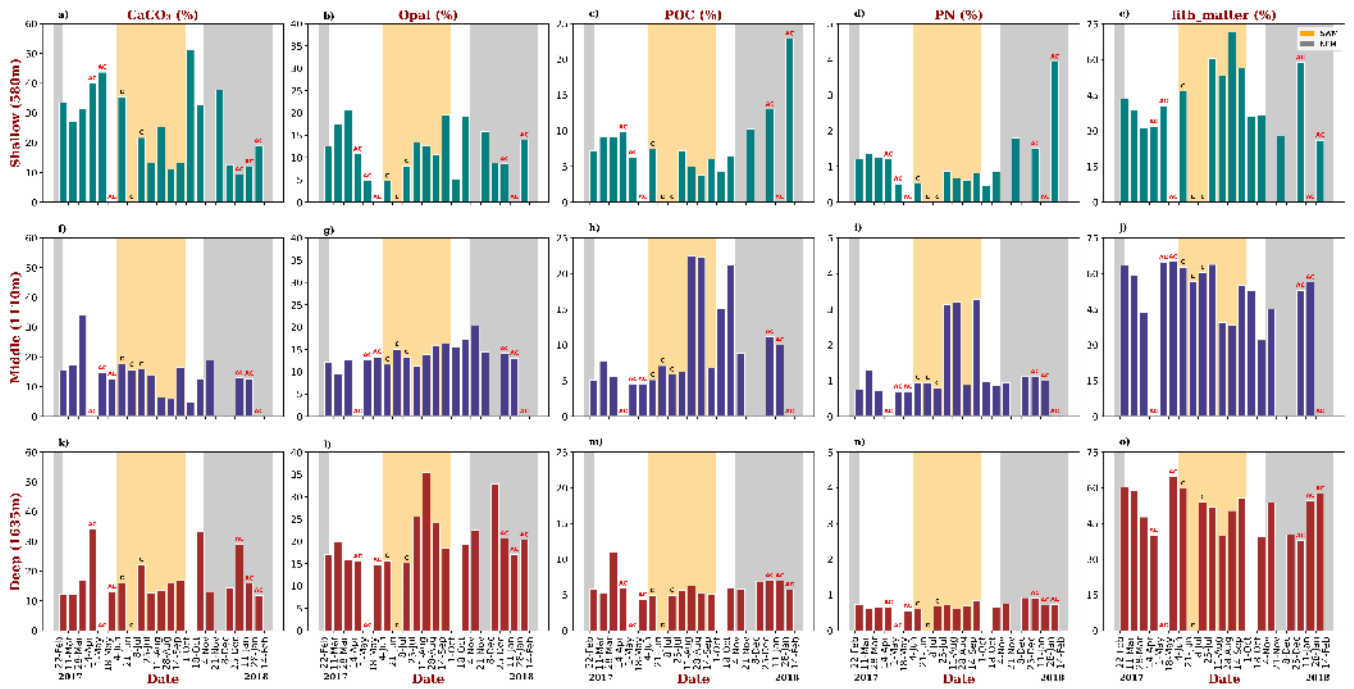


Figure 7. Seasonal variations of $\text{CaCO}_3\%$, Opal%, POC%, PN% and lithogenic matter% in the shallow (a-e), middle (f-j) and deep (k-o) traps in the BoBST from February 2017 to February 2018. Cyclonic (C) and anti-cyclonic (AC) eddies are shown and SWM and NEM are denoted as shaded boxes.

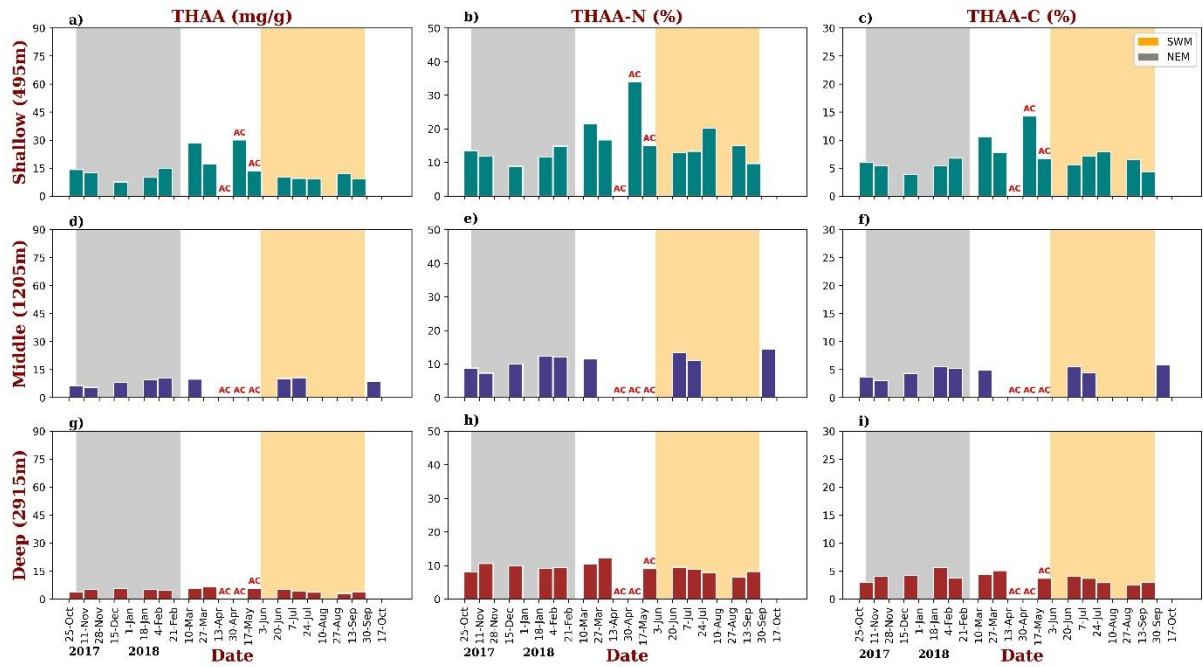


Figure. 8 Seasonal variations of THAA (mg/g), THAA-N (%) and THAA-C (%) in the shallow (a-c), middle (d-f) and deep (g-i) traps in the NEAST from October 2017 to September 2018. Cyclonic (C) and anti-cyclonic (AC) eddies are shown and SWM and NEM are denoted as shaded boxes.

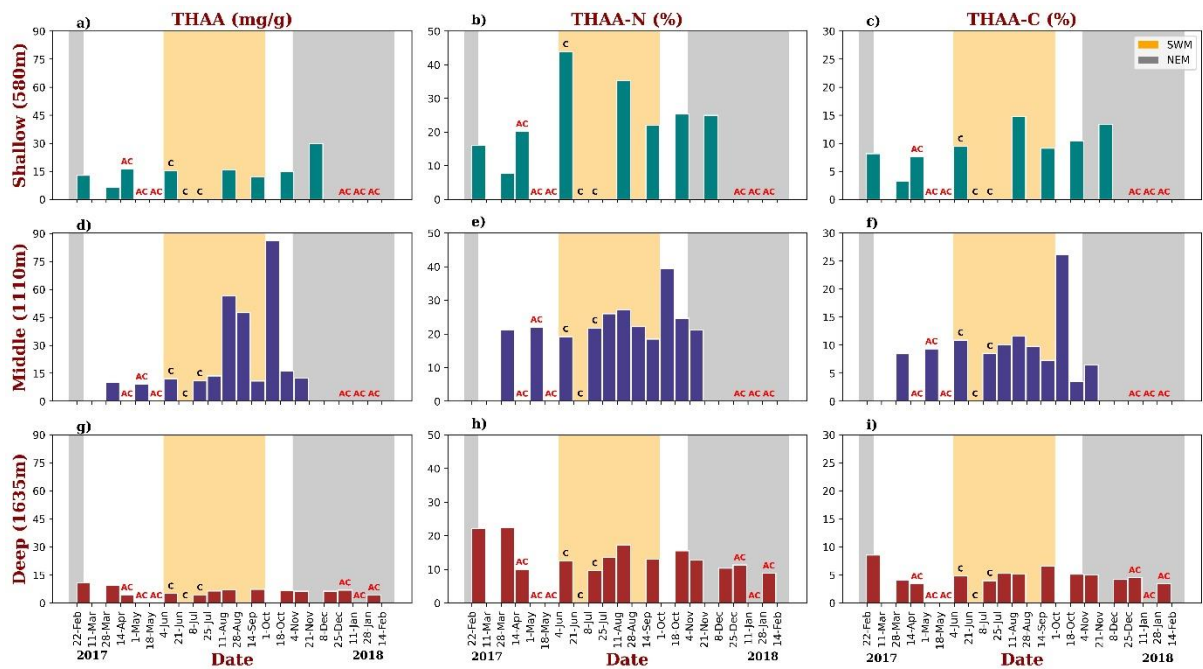


Figure 9. Seasonal variations of THAA (mg/g), THAA-N (%) and THAA-C (%) in the shallow (a-c), middle (d-f) and deep (g-i) traps in the BoBST from February 2017 to February 2018. Cyclonic (C) and anti-cyclonic (AC) eddies are shown and SWM and NEM are denoted as shaded boxes.

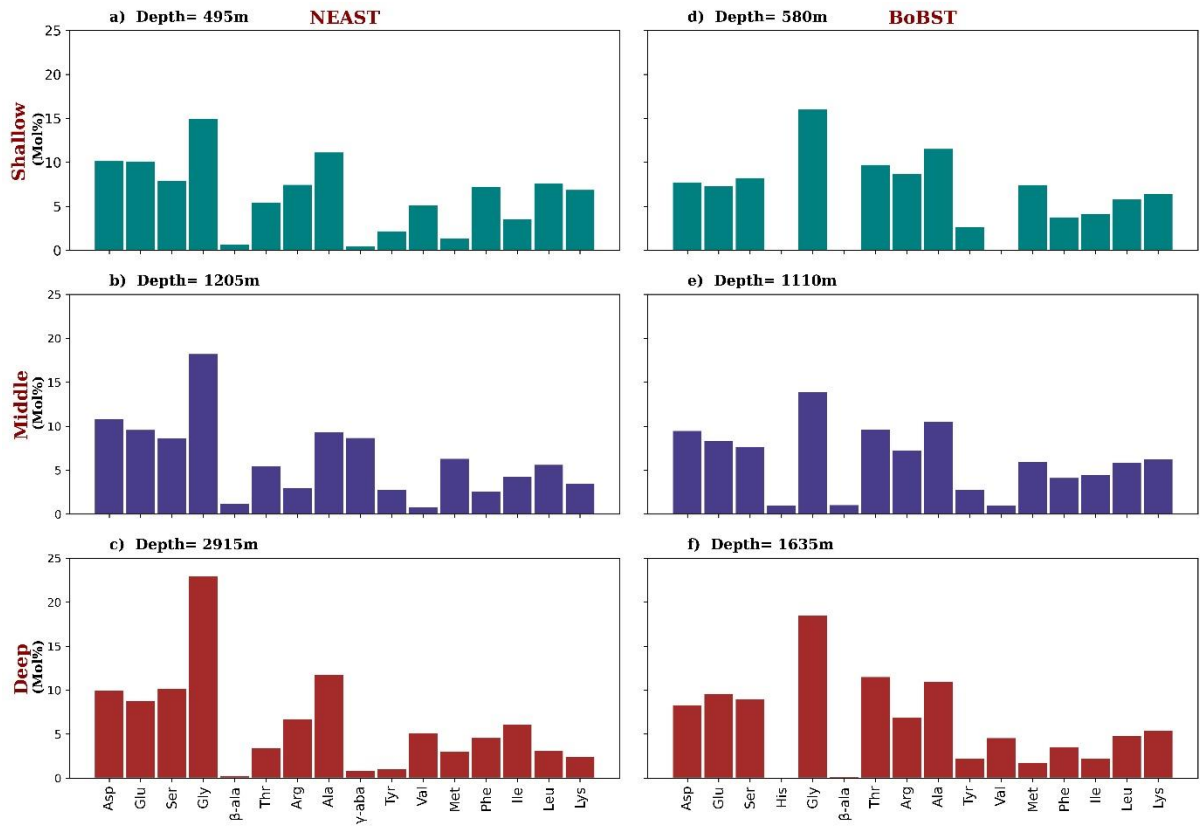


Figure 10. Average mol% of amino acid in the (a) shallow, (b) middle and (c) deep traps in the NEAST from October 2017 to September 2018 (LHS); and (d) shallow, (e) middle and (f) deep traps in the BoBST from February 2017 to February 2018 (RHS).

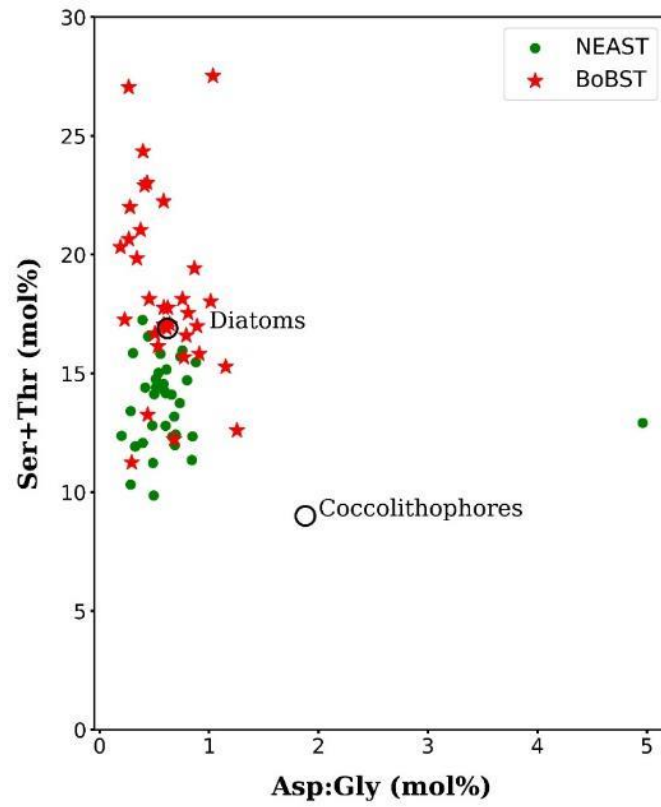


Figure 11. A plot of Ser+Thr (mol%) against Asp:Gly (mol%) in both NEAST and BoBST samples. The diatom and coccolithophore regions are marked based on Müller et al. (1986) and Salter et al. (2010).

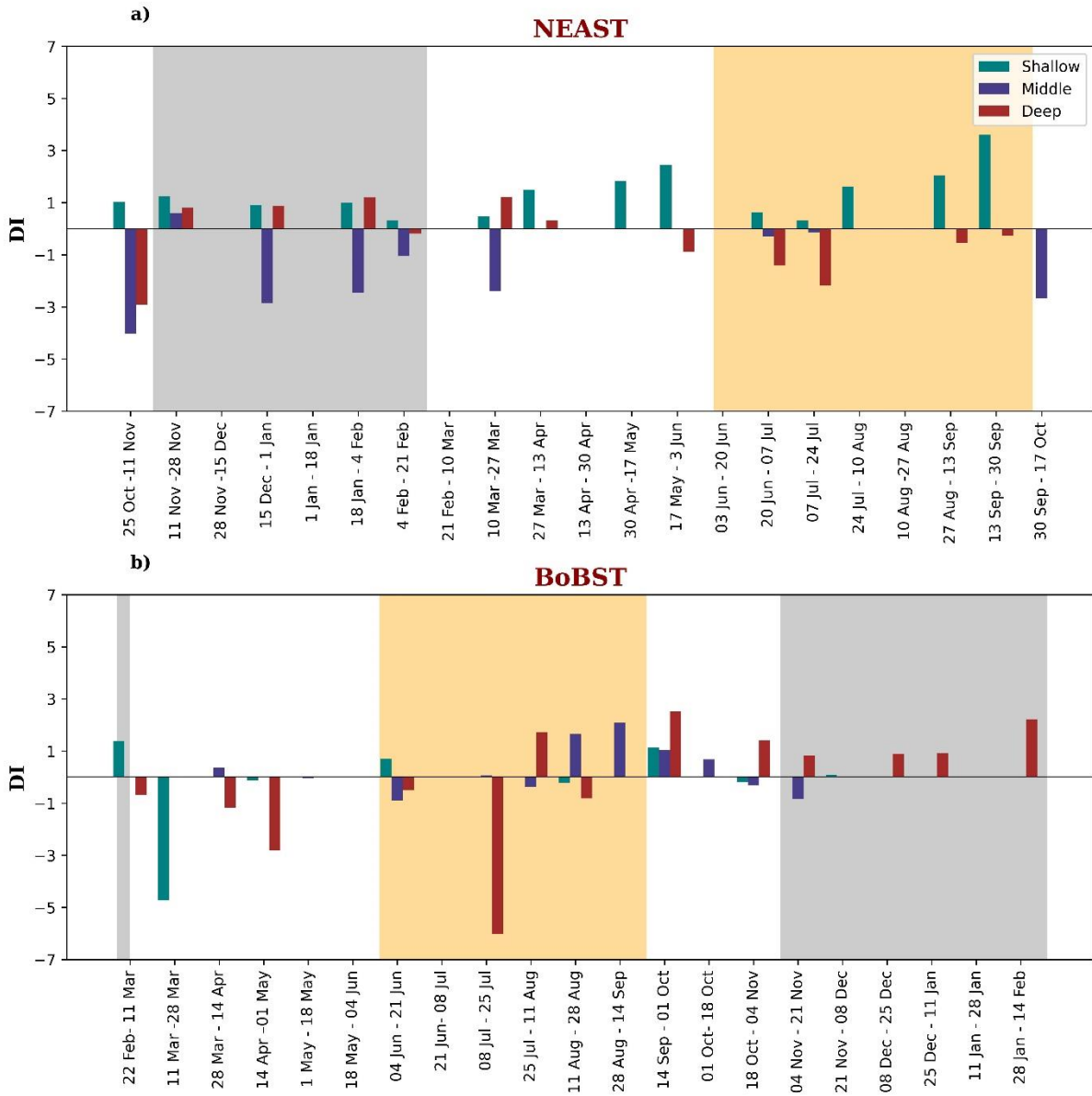


Figure 12. The degradation index (DI) in the shallow, middle, and deep traps in the (a) NEAST and (b) BoBST. The SWM and NEM are denoted as shaded boxes.